Journal of Medicinal Chemistry

pubs.acs.org/jmc Article

Beyond the Rule of 5: Impact of PEGylation with Various Polymer Sizes on Pharmacokinetic Properties, Structure−Properties Relationships of mPEGylated Small Agonists of TGR5 Receptor

Vanessa Hoguet,[#] Manuel Lasalle,[#] Mathieu Maingot, Geoffroy Dequirez, Rajaa Boulahjar, Florence Leroux, Catherine Piveteau, Adrien Herledan, Alexandre Biela, Julie Dumont, Oscar Chávez-Talavera, Loïc Belloy, Isabelle Duplan, Nathalie Hennuyer, Laura Butruille, Sophie Lestavel, Emmanuel Sevin, Maxime Culot, Fabien Gosselet, Bart Staels, Benoit Deprez,[*] Anne Tailleux,[◊] and Julie Charton[*,◊]

Cite This: *J. Med. Chem.* 2021, 64, 1593−1610 Read Online

ACCESS | Metrics & More | Article Recommendations | Supporting Information

ABSTRACT: PEGylation of therapeutic agents is known to improve the pharmacokinetic behavior of macromolecular drugs and nanoparticles. In this work, we performed the conjugation of polyethylene glycols (220−5000 Da) to a series of non-steroidal small agonists of the bile acids receptor TGR5. A suitable anchoring position on the agonist was identified to retain full agonistic potency with the conjugates. We describe herein an extensive structure−properties relationships study allowing us to finely describe the non-linear effects of the PEG length on the physicochemical as well as the *in vitro* and *in vivo* pharmacokinetic properties of these compounds. When appending a PEG of suitable length to the TGR5 pharmacophore, we were able to identify either systemic or gut lumen-restricted TGR5 agonists.

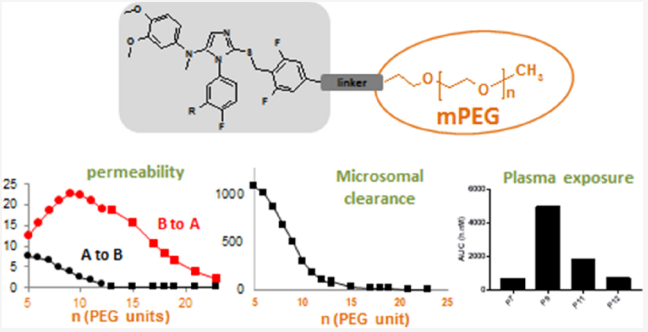

INTRODUCTION

Pegylation in Drug Discovery. Polyethylene glycol (PEG) polymers are composed of linear or branched repeating units of ethylene glycol. PEG is biocompatible, highly soluble, and FDA-approved for human use. Although there is increasing awareness of allergic reactions to PEGs, which must be kept in mind when designing new PEGylated compounds, PEGs are usually safe and widely used in foods, cosmetics, and drugs. Conjugation of polyethylene glycol to therapeutic agents is a commonly explored strategy to modulate the pharmacokinetic properties of drugs and thereby to improve their therapeutic effect. Initially, this strategy was mainly used for macromolecular drugs such as proteins, enzymes, nanoparticles, oligonucleotides, or antibodies and led to the commercialization of several drugs since 1990.[1−7] Most of these drugs, as well as those in development are macromolecules modified with large PEG (5−40 kDa). Nevertheless, PEGylation of small "drug-like" molecular agents is an emerging strategy to improve or enable novel therapeutics.[8−10]

Literature is rich in pharmacokinetics (PK) studies for large biomolecules coupled to large PEG (5−40 kDa).[11−13] However, the impact of PEGylation of small molecules with chains <5000 Da on PK properties remains largerly unknown. In addition, in the case of small molecules, PEGylation is more likely to mask a large proportion of the pharmacophore and leads to drastic loss of affinity due to steric hindrance than in the case of proteins and nucleic acids. Thus, accurate knowledge of structure−activity relationships of the parent compound and size and architecture of the PEG are crucial to address the challenge of the optimized balance between PD and PK.[14]

We will present here detailed *in vitro* and *in vivo* nonlinear structure−properties relationships in a series of TGR5 (Takeda G protein-coupled receptor 5) agonists aminothioimidazoles PEGylated with linear methoxy PEG (mPEG) of various lengths (220−5000 Da).

PEGylation of TGR5 Agonists. TGR5 (also known as GPBAR-1, GPR131, and M-BAR) is a G protein-coupled receptor responsive to bile acids identified in 2002.[15] TGR5

Received: October 9, 2020
Published: January 20, 2021

https://dx.doi.org/10.1021/acs.jmedchem.0c01774
J. Med. Chem. 2021, 64, 1593−1610

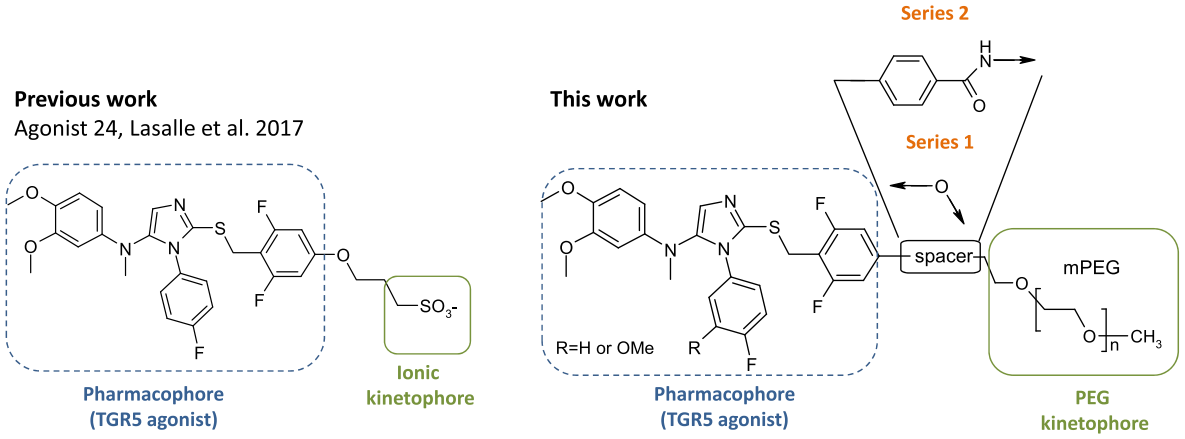

Figure 1. Previously described TGR5 agonist **24** and general structure of the PEGylated TGR5 agonists of this work.[21]

Scheme 1. Synthetic Route to 1 and 2[a]

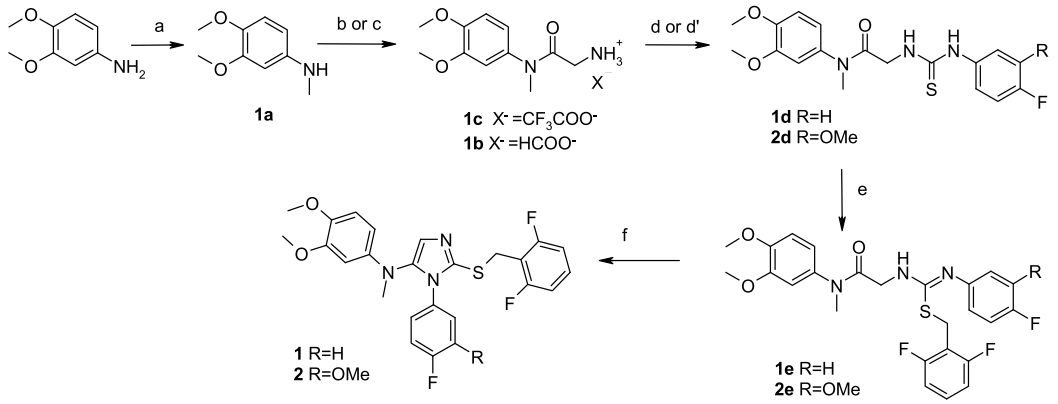

[a]Reagents and conditions: (a) (i) paraformaldehyde, MeONa, room temp., 16 h, (ii) $NaBH_4$, MeOH, reflux, 1−3 h, 77%; (b) (i) Boc-Gly-OH, T3P, DIEA, EtOAc, room temp., 30 min to 48 h, 100%, (ii) TFA(30%)/DCM, room temp., 30 min, 100%; (c) (i) chloroacetyl chloride, DIEA, CH_2Cl_2, 0 °C, 30 min, (ii) aq. NH_3, EtOH, 65 °C, 1 h, then HCOOH, 75% (over two steps); (d) 4-fluorophenylisothiocyanate, NEt_3, EtOH, room temp., 15 min, 76%; (d′) 4-fluoro-3-methoxy-aniline, TCDI, NEt_3, dioxane, room temp. to 60 °C, overnight, 49%; (e) 2-bromomethyl-1,3-difluorobenzene, NaI, K_2CO_3, CH_3CN, room temp., 16 h, 91%; (f) T3P, DIEA, EtOAC, 150 °C (μW), 10−40 min, or reflux, 24 h, 33−63%.

activation has been shown to trigger the secretion of intestinal glucagon-like peptide-1 (GLP-1) by colonic L cell[16] and enhanced energy expenditure.[17] It has recently become an attractive target for the treatment of type 2 diabetes and its metabolic complications. *In vivo*, to exert their GLP-1 secretagogue action and provide the expected antidiabetic effect, TGR5 agonists do not need to reach the systemic circulation. Indeed, they can stimulate GLP-1 secretion by activation of TGR5 expressed on the enteroendocrine L cells of the intestinal epithelium. Unwanted side effects triggered by activation of TGR5 in gallbladder, heart, and skin were reported by investigators working with systemic TGR5 agonists in preclinical models.[18−20] Consequently, the lowest possible, subpharmacological, systemic exposure is desirable.

Our team has previously described a new class of potent 5-amino-2-thio-imidazole TGR5 agonists.[21] In this previous work, to limit systemic exposure after oral administration, our TGR5 agonists were designed as chimeric compounds composed of a TGR5 pharmacophore linked to an ionic kinetophore.[21] The kinetophore concept, introduced in 2006, refers to a highly polar and/or large chemical moiety tethered to a pharmacologically active compound, meant to prevent absorption through the intestinal epithelium.[22,23] Amongst the possible "large and highly polar" kinetophore moieties, we decided to use, in this work, mPEG of various lengths as a single coupling chemistry can be used to produce structures of very different sizes and because we assumed that the large negative contribution of the PEG to logD could easily reduce intestinal absorption.

One of the milestones in the PEGylation strategy was the identification of a "mute" position on the pharmacophore part where linking such bulky and polar groups would not impact interactions with the target. Furthermore, each ethylene glycol in PEG binds to several water molecules (up to three per monomeric unit) leading to a solvated PEGylated structure much larger than a molecule of similar molecular mass.[1] During the optimisation of potency of our 5-amino-2-thioimidazoles,[21] we produced a detailed SAR and identified a proper position to link the methoxy PEG (mPEG) kinetophore with limited potency loss (Figure 1). The mPEGs were coupled directly to the parent compound (series 1) or through a benzamide linker to put the kinetophore farther away from the ligand−receptor interface (series 2).

RESULTS AND DISCUSSION

Chemistry. The synthesis of the 5-amino-2-thio-imidazole unconjugated parent compounds **1** and **2** was performed

https://dx.doi.org/10.1021/acs.jmedchem.0c01774
J. Med. Chem. 2021, 64, 1593−1610

Scheme 2. Synthetic Route to P3−P6[a]

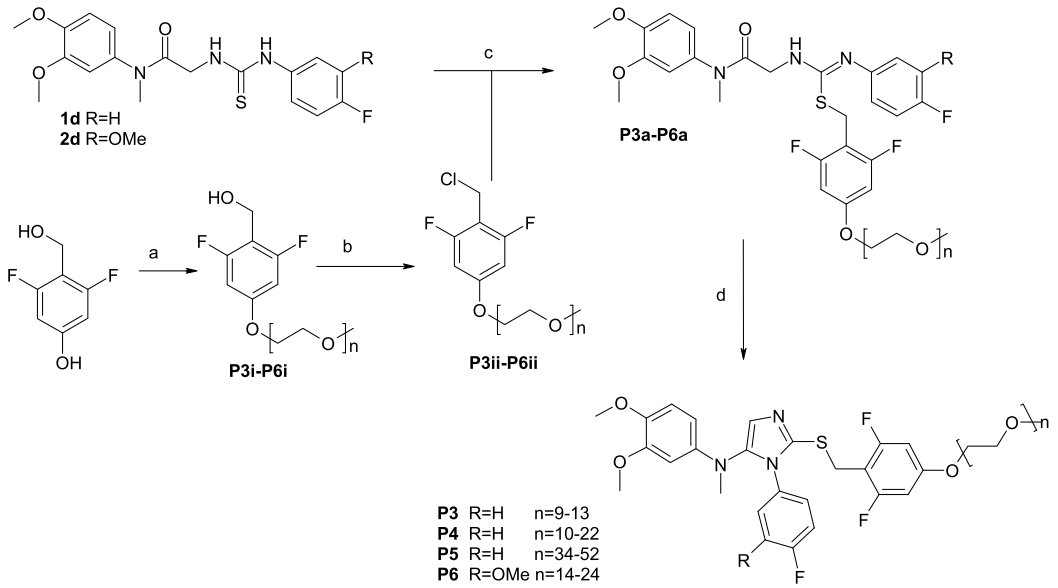

[a]Reagents and conditions: (a) poly(ethylene glycol) methyl ether tosylate (average Mn = 600, 900, and 2000 g/mol), K_2CO_3, acetonitrile, reflux, overnight, 61−100%; (b) TEA, mesyl chloride, DCM, room temp., overnight, 100%; (c) **P3ii−P6ii**, NaI, K_2CO_3, CH_3CN, room temperature, overnight, 17−47%; (d) T3P, DIEA, EtOAC, 150 °C (μW), 10−40 min, or reflux (classical heating), 24 h, 13−27%.

Scheme 3. Synthetic Route to P8 and P10[a]

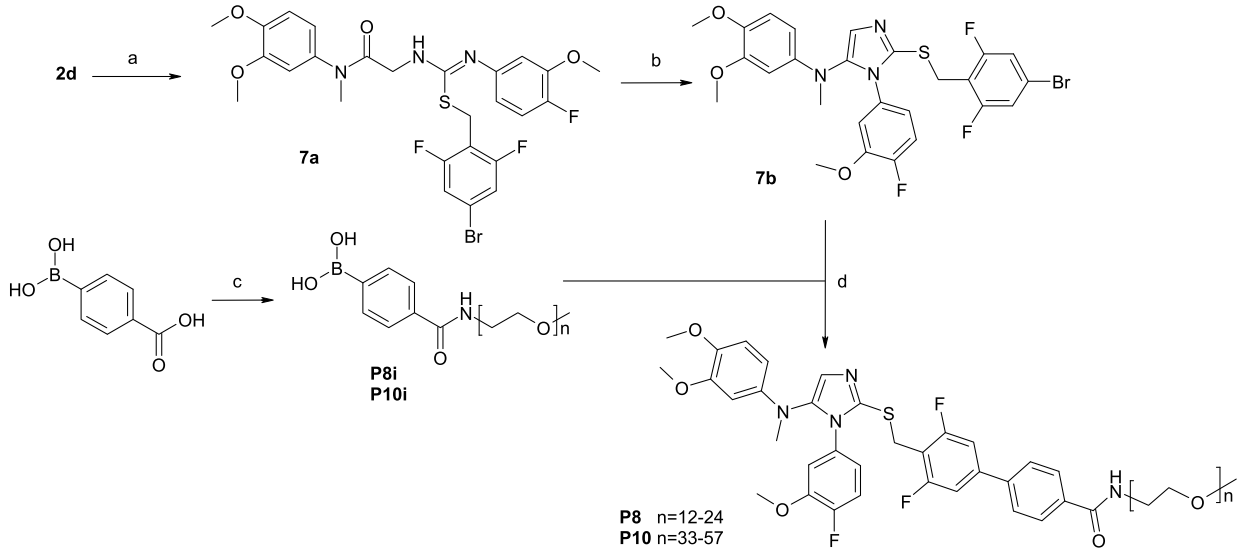

[a]Reagents and conditions: (a) 5-bromo-2-(chloromethyl)-1,3-difluoro-benzene, NaI, K_2CO_3, acetonitrile, room temp., overnight, 98%; (b) T3P, DIEA, EtOAc, 150 °C (μW), 10 min, 100%; (c) 2-[2-methoxypolyethyleneglycoxy]ethanamine (average Mn = 750 and 2000 g/mol), TEA, DCC, HOBt, DCM, room temp., overnight, 64−66%; (d) **P8i** or **P10i**, Cs_2CO_3, $Pd(PPh_3)_4$, H_2O/DME/EtOH, 100 °C (μW), 10 min, 43−47%.

following procedures previously described and is presented in Scheme 1.[21,24]

For clarity of presentation, to differentiate easily monodisperse and polydisperse PEGylated conjugates, a P was added to the number of the polydisperse mPEG conjugates. Compounds **P3** to **P6** (series 1) were obtained by the same synthetic pathway starting from the thiourea intermediates **1d** and **2d** (Scheme 2). PEGylated *S*-benzylisothioureas **P3a−P6a** were obtained by alkylation of **1d** and **2d** with mPEG benzyl chloride intermediates (**P3ii−P6ii**). After cyclization and HPLC purification, compounds **P3−P6** were obtained as polydisperse mixtures and characterized by LCMS to determine the number of ethylene oxide units (n).

As for series 2, two synthetic pathways were investigated. In the first route, the mPEG moiety was introduced on a boronic acid intermediate and coupled to the pharmacophore part via a Suzuki reaction to give compounds **P8** and **P10** (Scheme 3). In a more convenient and convergent route, the mPEG part was introduced in the last step of the synthesis by forming an amide bond with commercial polydisperse (mPEG-NH_2, average Mn = 500, 750, 2000, and 5000 g/mol) or monodisperse PEGylated amines (n = 5, 7, 9, 11, 16, 24, 36) and biphenylcarboxylic acid intermediate **7c**. This second

https://dx.doi.org/10.1021/acs.jmedchem.0c01774
J. Med. Chem. 2021, 64, 1593−1610

Scheme 4. Synthetic Route to P7−P12 and 13−19[a]

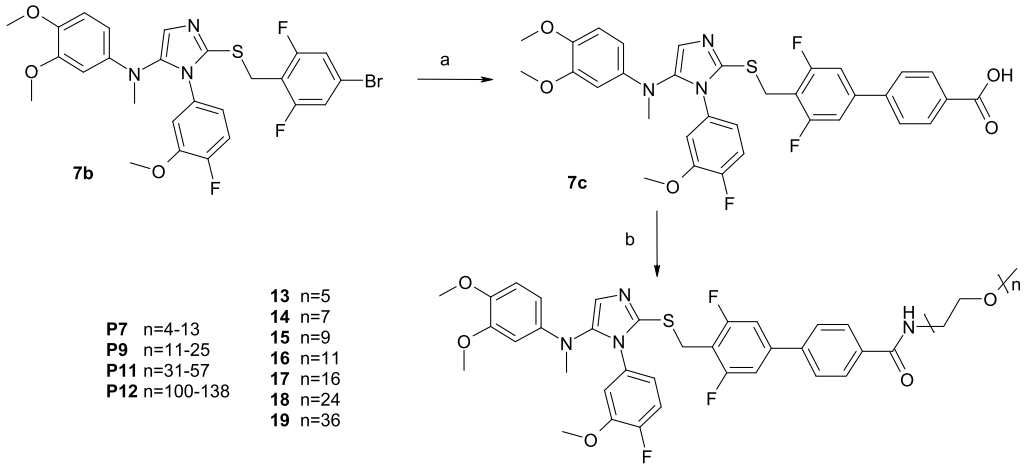

[a]Reagents and conditions: (a) 4-carboxyphenylboronic acid, Cs_2CO_3, $Pd(Ph_3P)_4$ or $PdCl_2dppf$, H_2O/DME/EtOH, 100 °C (μW), 10 min, 52%; (b) mPEG-NH_2 (average Mn = 500, 750, 2000, and 5000 g/mol) or mPEGn-NH_2, TEA, DCC, or DIC, HOBt, DCM, room temp., overnight.

Table 1. *In Vitro* Activities of Compounds 1, 2, and P3−P6 (Series 1)

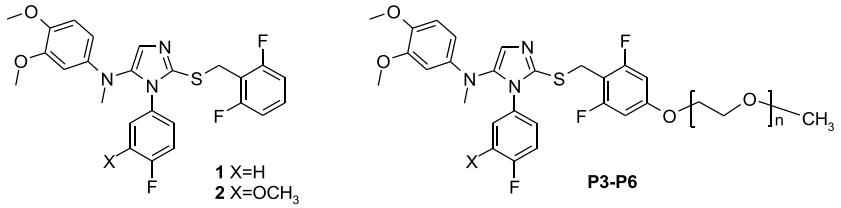

example	X	*n*	EC_{50} (nM)[a] hTGR5	EC_{50} (nM)[a] mTGR5
1	H		35 [22−54]	0.8 [0.5−1.4]
P3	H	9−13	166 [133−208]	18 [13−26]
P4	H	10−22	580 [536−628]	29 [25−33]
P5	H	34−52	1230 [1145−1322]	68 [62−75]
2	OCH_3		20 [13−30]	0.8 [0.2−3.4]
P6	OCH_3	14−24	330 [306−349]	26 [22−30]

[a]CRE-driven luciferase reporter assays in TGR5-transfected HEK293 cells. Units are nM for EC50. EC50 values are reported with their 95% confidence intervals in brackets.

route afforded for polydisperse compounds **P7**, **P9**, **P11**, and **P12** and seven monodisperse compounds **13−19** (Scheme 4).

***In Vitro* Studies.** *Biological Activity.* The *in vitro* potencies of the mPEGylated compounds were first compared to their unconjugated counterparts **1** and **2**. EC_{50}s were measured on both human and murine receptors in a CRE-driven luciferase reporter assay in TGR5-transfected HEK293 cells (Tables 1 and 2).

The introduction of a mPEG moiety directly on the difluorophenyl ring (**P3−P6**) led to a PEG size-dependent decrease in potency on both human and murine receptors. However, potencies remained in the nanomolar range on the murine receptor for all sizes. Potency was slightly better on the human receptor (**P6** *versus* **P4**) when starting from unconjugated parent compound **2** (X = OCH_3).

As expected, the addition of a larger and more rigid spacer (series 2) aiming at reducing the steric interference of the mPEG part on the pharmacophore-target interaction allowed a 2-fold gain of potency on both receptors (**P9** versus **P6**). Interestingly, the use of two different synthetic routes gave the target compound with highly similar PEG size distribution (compounds **P8** (n = 12−24) versus **P9** (n = 11−25) and **P10** (n = 33−57) versus **P11** (n = 31−57)) and the same

Table 2. *In Vitro* Activities of Compounds 2, P7, P9, P11, P12, 13−19 (Series 2)

example	*n*	EC_{50} (nM)[a] hTGR5	EC_{50} (nM)[a] mTGR5
polydisperse			
2		20 [13−30]	0.8 [0.2−3.4]
P7	4−13	60 [48−75]	5 [4−6]
P9	11−25	145 [129−163]	13 [11−15]
P11	31−57	515 [442−601]	25 [21−29]
P12	100−138	1102 [940−1291]	63 [59−68]
monodisperse			
13	5	99 [81−122]	6 [5−7]
14	7	99 [76−128]	10 [9−11]
15	9	122 [106−140]	13 [12−14]
16	11	120 [107−135]	13 [12−14]
17	16	609 [441−841]	30 [26−36]
18	24	735 [523−1032]	39 [31−49]
19	36	1527 [1126−2073]	50 [35−70]

[a]CRE-driven luciferase reporter assays in TGR5-transfected HEK293 cells. Units are nM for EC50. EC50 values are reported with their 95% confidence intervals in brackets.

https://dx.doi.org/10.1021/acs.jmedchem.0c01774
J. Med. Chem. 2021, 64, 1593−1610

Table 3. *In Vitro* Physicochemical and ADME Parameters of PEGylated Compounds and Their Parent Analogs

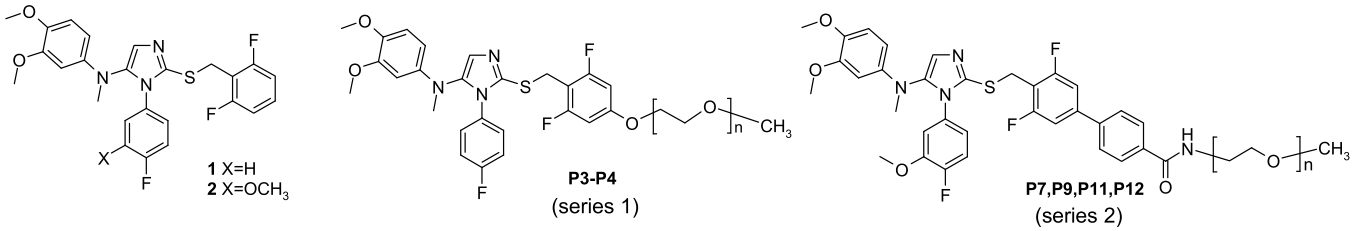

Cpd	*n* (PEG unit)	MW (g/mol)	solubility (μM)[a]	LogD$_{7.4}$	Cl$_{int}$[b]	P$_{app\ A\text{-}B}$[c]	P$_{app\ B\text{-}A}$[c]	efflux ratio
1		485	6.3	3.5	1287	5.3	5.5	1.0
P3	9−13	911−1087	181	2.1	528	8.4	17	2.1
P4	10−22	955−1483	>200	1.5	34	<0.2	25	>125
2		516	8.8	3.97	1254	9.3	8.5	0.9
P7	4−13	824−1220	151	3.42	524	4.9	19.5	4.0
P9	11−25	1132−1748	>200	1.58	17	<0.02	9.1	>455
P11	31−57	2012−3156	>200	−1.53	8	<0.12	<0.03	nd
P12	100−138	5048−6720	>200	−1.58	11	nd	nd	nd

[a]Solubility measured in PBS pH 7.4 starting from a 10 mM solution in DMSO of the compound (Method A). [b]Cl$_{int}$: intrinsic clearance measured on male mouse microsomes (μL/min/mg proteins). [c]Permeability on a Caco-2 cell monolayer. "A-B" indicates the transport from the apical side to the basolateral side; "B-A" indicates the transport from the basolateral side to the apical side. Permeability is expressed in 10^{-6} cm/s. Permeability classification: low, P$_{app}$ < 2 × 10^{-6} cm/s; high, P$_{app}$ > 20 × 10^{-6} cm/s. Compounds recovery >75% in all experiments except for **P7** in P$_{app\ A\text{-}B}$ experiment (54%).

potencies. It is important to note that, while potency appears to be size-dependent, all conjugates (even the larger PEG conjugate **P12**, *n* > 100) retained their full TGR5 agonist efficacy in the *in vitro* reporter assay.

Physicochemical and In Vitro ADME properties. *In vitro* ADME studies were then performed to further characterize the profile of the conjugates. Solubility, lipophilicity, metabolic stability, and permeability were measured for both series of polydisperse PEG conjugates (**P3** and **P4** and **P7**, **P9**, **P11**, and **P12**, Table 3).

As expected, the PEGylation of the small TGR5 agonists substantially alters their physicochemical and ADME properties in a size-dependent manner (Table 3). The introduction of a PEG moiety strongly improved solubility in both series 1 and 2 in agreement with the decrease in lipophilicity (LogD7.4). Introduction of the shorter PEG (**P3** and **P7**) has a moderate effect on the microsomal stability with a decrease by a factor 2 of the intrinsic clearance compared the parent compounds (**1** and **2**). In contrast, the longer PEG confers protection against oxidative metabolism to the conjugate compounds (**P4**, **P9**, **P11**, and **P12**). The impact of PEGylation (PEG ≤5 kDa) of the TGR5 agonists on intestinal permeability was assessed *in vitro* in a Caco-2 monolayer permeability assay. As can be seen in Table 3, compounds **P3** and **P7** (*n* ≤ 13) retain a substantial permeability (2 × 10^{-6} cm/s < P$_{app}$A-B < 20 × 10^{-6} cm/s), whereas conjugates from both series with larger PEG (**P4**, **P9**, **P11**, and **P12**) are classified as poorly permeable (P$_{app}$A-B < 2 × 10^{-6} cm/s). Surprisingly, the very low transepithelial permeability from apical to basal side of **P4** and **P9** is not due to a poor membrane crossing ability (P$_{app}$B-A > 2 × 10^{-6} cm/s) but to a very high efflux (efflux ratio > 100), showing that they are substrates of efflux pumps despite their high molecular weight. Conjugates of higher size (**P11** and **P12**) however are unable to enter the cell neither through passive diffusion nor active transport (P$_{app}$A-B and P$_{app}$B-A < 2 × 10^{-6} cm/s).

We next refined the structure−properties relationships by measuring *in vitro* ADME properties for individual compounds in the polydisperse compounds of series 1 (**P3** and **P4**) and 2 (**P7** and **P9**). The effect of PEG size on oxidative metabolism was investigated more finely (Figure 2).

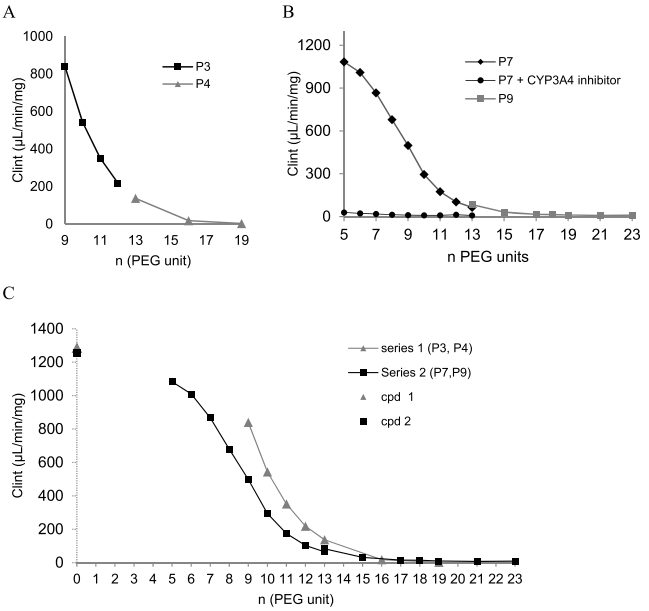

Figure 2. Effect of the number of PEG units (*n*) on microsomal stability. (A) Intrinsic clearance Cl$_{int}$ (μL/min/mg) for compounds **P3** and **P4** (series 1) as a function of size. (B) Intrinsic clearance Cl$_{int}$ (μL/min/mg) for compounds **P7** and **P9** (series 2) with or without CYP3A4 inhibitor (ketoconazole, 5 μM). (C) Intrinsic clearance Cl$_{int}$ (μL/min/mg) for series 1 and 2.

In both series, we can see again a clear dependence of the oxidative metabolism on the PEG size (Figure 2A,C) and the cytochrome 3A4 appeared to be the main isoform in the metabolism of our PEGylated conjugates since the intrinsic clearance was reduced drastically in presence of ketoconazole, a CYP3A4 inhibitor (Figure 2B).

https://dx.doi.org/10.1021/acs.jmedchem.0c01774
J. Med. Chem. 2021, 64, 1593−1610

The apical to basolateral permeability decreases with the increase in PEG length. Interestingly enough, the PEG itself, despite its very large size compared to the original ligand and its important contribution to molecular surface, volume, and logD, does not impose a full control on membrane crossing ability and clearance over the properties of the naked ligand. Indeed, significantly different permeabilities are observed between series 1 and 2 for n below 13 PEG units. It is only when n reaches 13 that the permeability becomes very low in both series (Figure 3).

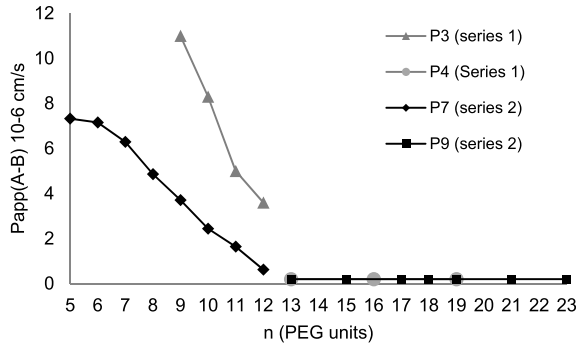

Figure 3. Apparent permeability on Caco-2 cell monolayer $P_{app\ A\text{-}B}$ (from the apical side to the basolateral side) for series 1 (gray, compounds **P3** and **P4**) and series 2 (black, compounds **P7** and **P9**) depending on the number of PEG units (for $n \geq 13$ P_{app}A-B < 0.2 × 10^{-6} cm/s).

Solubility, intestinal (Caco-2 cell monolayer), and blood–brain barrier (BBB) permeabilities were also measured for the monodisperse PEGylated analogs **13**–**19**. Permeability across brain-like endothelial cells (BLECs) were assessed on an *in vitro* human BBB model consisting of endothelial cells derived from $CD34^+$ cells co-cultivated with brain pericytes, thus acquiring a BLEC phenotype in 6 days. Values measured for monodisperse species are in very good agreement with those measured for mixtures. A dramatic increase in the solubility was observed between compounds **14** (161 μM) and **15** (>50,000 μM) with only two PEG units difference between both compounds (n = 7 and n = 9, respectively). We confirmed the decrease in the permeability in a PEG length-dependent manner. The BBB permeability (endothelial permeability coefficient ($Pe_{A\text{-}B}$)) was very low for all compounds ($Pe_{A\text{-}B}$ < 1 × 10^{-3} cm/min), showing that PEGylation can be used to exclude compounds from certain tissues, such as the central nervous system by impeding crossing of the blood–brain barrier (Table 4).

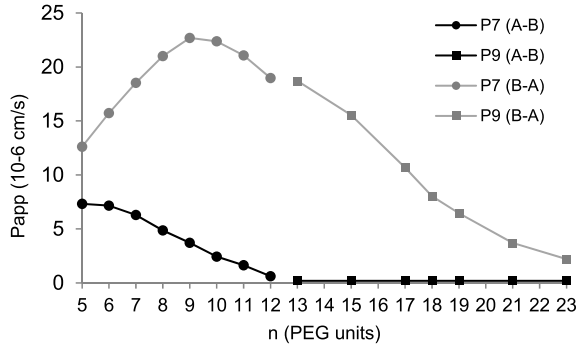

Figure 4. Apparent permeability on Caco-2 cell monolayer: A-B (from apical to basolateral) and B-A (from basolateral to apical) for compounds **P7** and **P9** depending on the number of PEG units. Permeability is expressed in 10^{-6} cm/s.(for $n \geq 13$ PappA-B < 0.2 × 10^{-6} cm/s).

As for compound **P9** (n = 11–25), a very high efflux ratio (>450) was obtained for compound **17** (n = 16) in the Caco-2 assay. Caco-2 cells express several efflux transporters such as P-glycoprotein (P-gp, ABCB1), breast cancer resistance protein (BCRP, ABCG2), and members of multidrug resistance-associated protein family (MRPs, ABCCs). To determine if the PEGylated conjugates are substrates or inhibitors of efflux pumps, we loaded Caco-2 cells with specific substrates of these pumps (rhodamine 123 for P-gp/BCRP and CMFDA for MRPs) and investigated effect of these compounds on cellular efflux of these substrates[25] (Figure 5).

Altogether, these results in Caco-2 cells and BLECs confirmed that PEGylated conjugates do interact with efflux transporters expressed by physiological barrier cells composing intestine or blood–brain barrier. Results of Figure 5 indicate that compound **2** is an inhibitor of P-gp/BCRP, whereas conjugation with PEG chains alleviates inhibition and increases

Table 4. Calculated and Measured ADME Paramaters of Monodisperse PEGylated Analogs

						apparent permeability on Caco-2 cell monolayer [c]			permeability across BLECs[d]
cpd	n	MW (g/mol)	solubility[a] (μM)	ALogP[b]	PSA (Å^2)[b]	$P_{app\ A\text{-}B}$	$P_{app\ B\text{-}A}$	efflux ratio	$Pe_{A\text{-}B}$
2		516	8.8	6.6	74	5.2	3.8	0.7	0.42
13	5	1354	3.2	5.2	149	4.1	6.0	1.5	0.50
14	7	1133	161	5.9	168	5.8	8.7	1.5	0.67
15	9	1045	>50,000	6.2	186	2.7	32.0	11.8	0.36
16	11	957	>50,000	6.4	205	0.5	33.3	74.1	0.21
17	16	869	>50,000	6.7	251	0.04	15.6	465.5	0.10
18	24	1706	>50,000	4,2	325	≤0.011	2.1	ND	0.09
19	36	2235	>50,000	2.6	435	≤0.015	0.07	ND	0.09

[a]Solubility measured in water starting from the powder of the compound (Method B) except for compound **2** (Method A). [b]Calculated parameter using Pipeline Pilot (Dassault Systems). PSA: polar surface area. [c]Permeability assessed on a Caco-2 cell monolayer. "A-B" indicates the transport from the apical side to the basolateral side; "B-A" indicates the transport from the basolateral side to the apical side. Apparent permeability (Papp) is expressed in 10^{-6} cm/s. Permeability classification: low, Papp < 2 × 10^{-6} cm/s; high, Papp > 20 × 10^{-6} cm/s. [d]Permeability across BLECs ($Pe_{A\text{-}B}$) is expressed in 10^{-3} cm/min. Permeability classification: low permeability, Pe < 1 × 10^{-3} cm/min. High permeability, Pe > 2 × 10^{-3} cm/min.

https://dx.doi.org/10.1021/acs.jmedchem.0c01774
J. Med. Chem. 2021, 64, 1593–1610

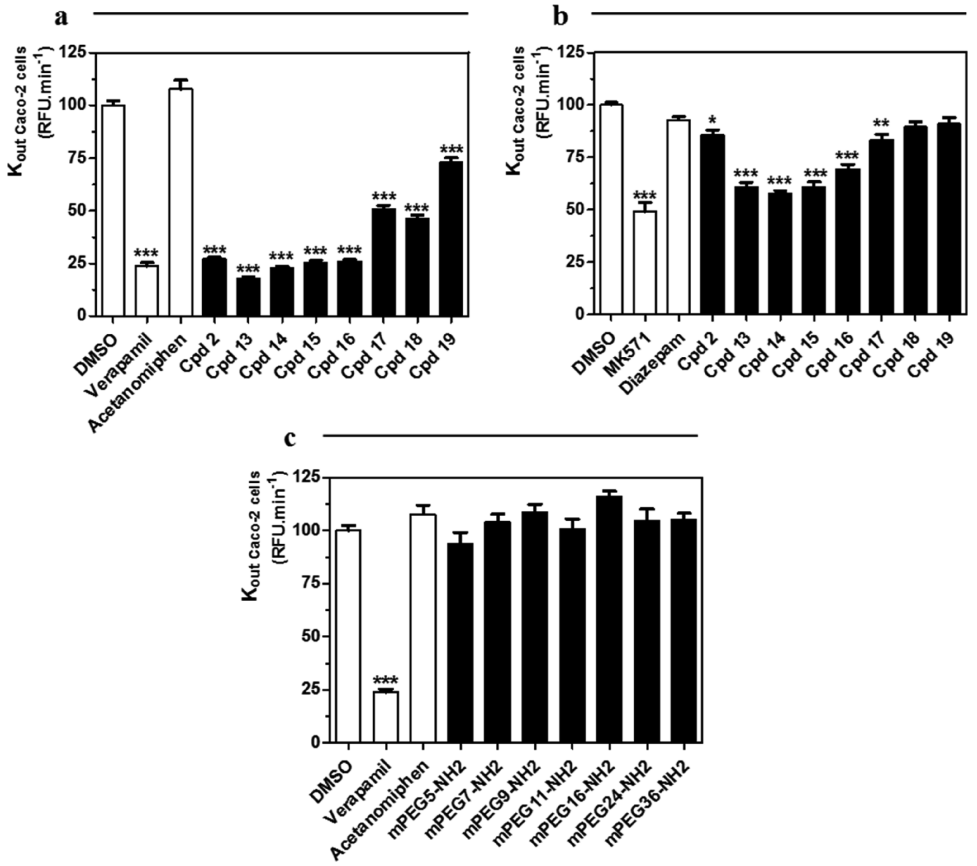

Figure 5. (a) Effect of PEGylated analogs on rate of excretion of rhodamine 123. (b) Effect of PEGylated analogs on the rate of excretion of CMFDA. (c) Effect of polyethylene glycol amine (mPEGn-NH_2) on the rate of excretion of rhodamine 123. Specific inhibitors for P-gp/BCRP (verapamil), MRPx (MK571) were used as positive control. Acetanomiphen and diazepam were used as negative controls. Data were represented as means + s.e.m. (n = 8−15), *p < 0.05, **p < 0.01, ***p < 0.001 (ANOVA−Dunnett test).

efflux accordingly. In contrast, compound **2** does not seem to interact with MRPx (no inhibition, no efflux). Interestingly, coupling with PEG induces inhibition of MRPx at small chain lengths while long chain lengths (n = 16−24) reduce interaction with the pumps as for P-gp and BCRP. Since basolateral to apical (B-A) permeability across Caco-2 could be influenced both by the ability of compounds to permeate cell membrane (passive permeability) and by their active efflux by transporters, this might explain the biphasic effect of the PEG chain length on the transport from basolateral to apical compartment (B to A) observed in Caco-2 cells for polydisperse conjugates (Figure 4). The decrease in permeability for PEGylated conjugates also observed in a human BBB model expressing these efflux pumps also supports this hypothesis.

***In Vivo* Studies.** Compounds of series 1 and 2 showing similar *in vitro* ADME properties, we selected compounds of series 2 for *in vivo* studies because they display higher potencies on both murine and human TGR5 activation. *In vivo* pharmacokinetic studies were performed to assess the impact of the PEG size on the exposure of some organs and tissues following oral administration by the polydisperse compounds of series 2. First, plasma and liver compound concentrations were measured (Figure 6). Second, as several TGR5 agonists are described to be highly excreted in bile, we were interested in measuring the concentrations of such large agonists in gallbladder (Figure 6). At last, in our research program aiming at targeting distal intestinal TGR5, data on the time course in the gut for the PEGylated conjugates were crucial for the proper design of *in vivo* pharmacodynamic experiments. Thereby, the concentrations of the conjugates in the different sections of the intestine were measured as a function of time after gavage to define their transit time and gut exposure (Figure 7).

In our series, plasma and liver exposure reach a moderate maximum for the intermediate size **P9** and remain very low for the other compounds (**P7**, **P11**, and **P12**).

Despite its very low permeability on Caco-2 cells (Papp < 0.02×10^{-6} cm/s), **P9** has a higher plasma and liver exposure after oral dosing than compound **P7**, expected to be more absorbed consistently with its higher permeability (Papp = 4.9×10^{-6} cm/s). This result could be explained by the better metabolic stability of **P9** (as observed *in vitro* on microsomes).

As we observed that some of our PEGylated conjugates are highly effluxed and substrates of some intestinal efflux transporters expressed in Caco-2 cells (P-gP), we were interested in exploring the effect of the PEG length on their biliary excretion. As can be seen in Figure 6, weak gallbladder exposure was observed for **P11** and **P12** while high concentrations of compounds **P7** and **P9** were measured.

PEG length also drastically impacts gut luminal exposure. In line with its permeability measured *in vitro* (Caco-2 assay), compound **P7** displays a very low exposure of the GI tract, that can be the result of an early and strong intestinal absorption compared to longer PEG conjugates. In contrast, high concentrations of **P9**, **P11**, and **P12** were measured in the

https://dx.doi.org/10.1021/acs.jmedchem.0c01774
J. Med. Chem. 2021, 64, 1593−1610

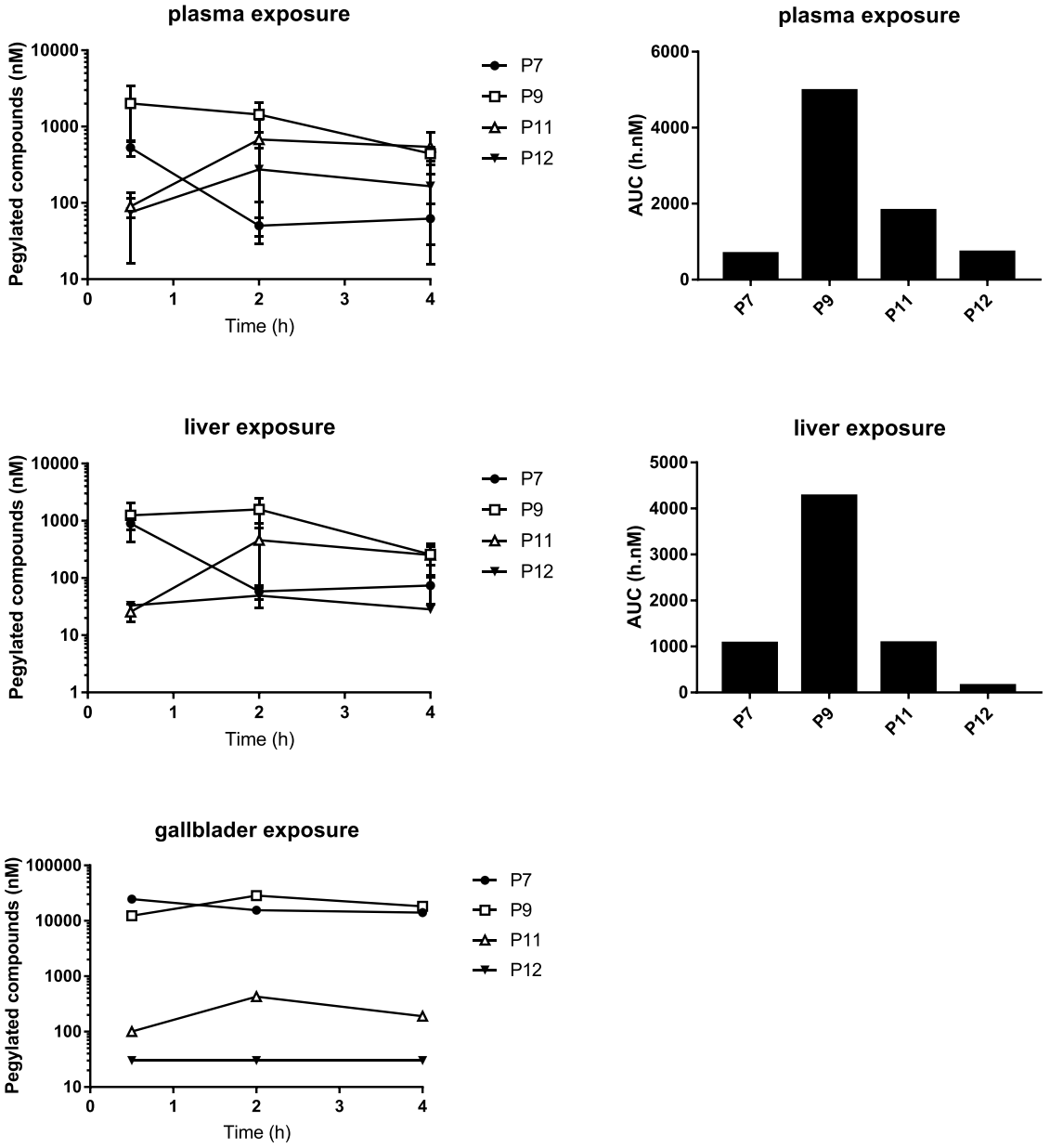

Figure 6. Plasma, liver, and gallbladder exposure in C57Bl6 mice following oral dosing (32 μmol/kg) of compounds **P7**, **P9**, **P11**, and **P12** (n = 3 mice/time points).

distal intestine (C > 500 μM) from 4 h after oral administration onward.

In all, these *in vitro* and *in vivo* PK studies on the different PEG conjugates allowed us to explore and fine-tune the impact of the PEGylation on the ADME profile of these compounds. As expected, we observed that solubility increased and lipophilicity decreased in a PEG length-dependent manner in both series 1 and 2. PEGylation, even with very short PEG, was in this project an efficient strategy to dramatically improve the solubility of the naked pharmacophores (from micromolar range for pharmacophore **2** to more than 50,000 μM for conjugates from n = 9, **15**−**19**, Table 4). Interestingly, we observed that short PEGs in both series 1 and 2 (**P3** and **P7**, $n \leq 13$, Cl_{int} around 500 μL/min/mg proteins) have a moderate impact on the microsomal stability (Cl_{int} around 1200 μL/min/mg proteins for the naked pharmacophores) while longer PEG efficiently protected the conjugates against oxidative metabolism (Cl_{int} < 20 μL/min/mg proteins for **P9**, **P11**, and **P12**). The impact of the spacer (series 1 and 2) on microsomal stability is significant for n < 13, but intrinsic clearance becomes very low for n above 13 units of PEG in both series (Figure 2C). Intestinal permeability and transport are also finely tuned by chosing the right PEG length. The intestinal absorption can be drastically reduced with nine or more PEG units (**15**−**19**, P_{app}A-B < 2 × 10^{-6} cm/s). It is important to remember that compounds **15**, **16**, and **17** (n = 9, 11, 16, respectively) display high permeability from the basolateral to apical side (B-A). Therefore, the low transepithelium permeability is not the result of a poor membrane crossing ability but rather that of their high efflux (efflux ratio = 465 for **17**). In contrast, **18** (n = 24) and **19** (n = 36) are unable to cross the membrane through passive diffusion nor active transport (very low P_{app}A-B and P_{app}B-A). It is worth nothing that PEGylation of the pharmacophore **2**, which is a substrate

https://dx.doi.org/10.1021/acs.jmedchem.0c01774
J. Med. Chem. 2021, 64, 1593−1610

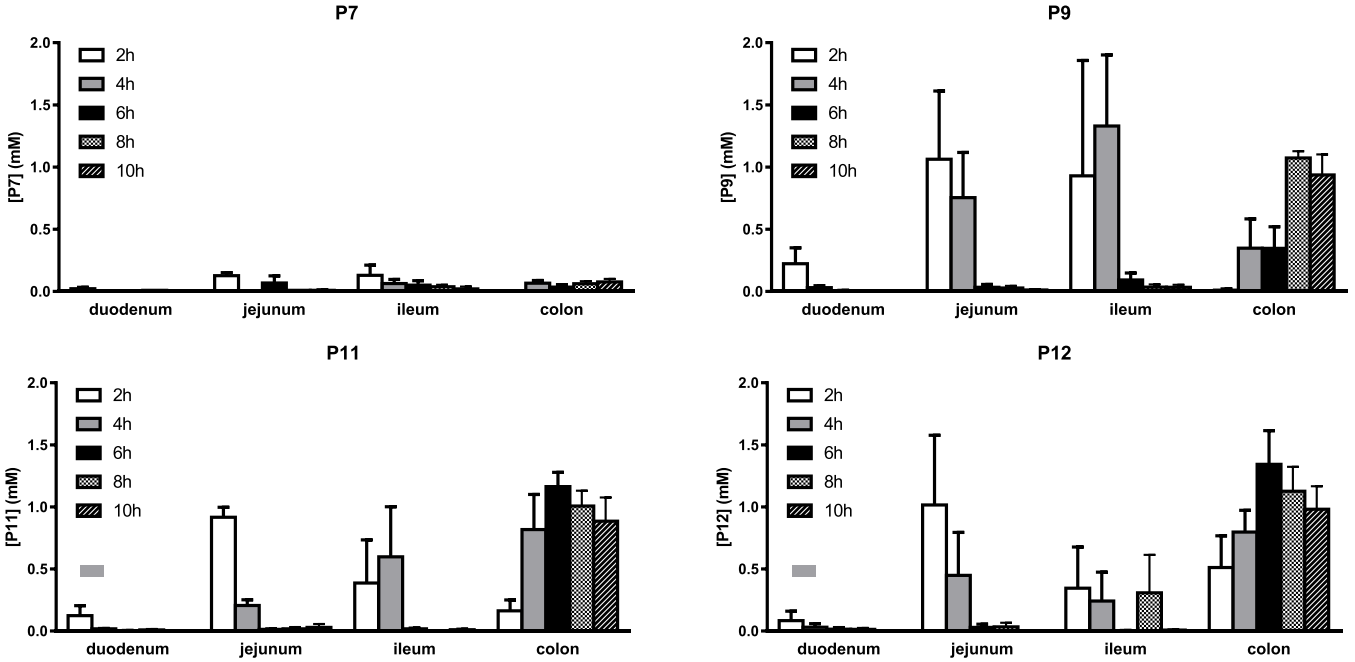

Figure 7. Time course of compounds **P7**, **P9**, **P11**, and **P12** concentrations in duodenum, jejunum, ileum, and colon of C57Bl6 mice, after a single oral administration (32 μmol/kg), mean ± s.e.m. (n = 3 mice/time points).

of the efflux pump P-gP/BCRP (Figure 5a), even with the longer PEG (**19**, n = 36, MW = 2235 g/mol), does not preclude the interaction of the conjugate with this transporter nor its ability to be transported. Interestingly, the mPEGn-NH_2 are not P-gP/BCRP substrate (Figure 5c) showing that the hydrophobic pharmacophore is required for the interaction with this efflux pump and the PEG moiety alone is not recognized by P-gp or BCRP.

The *in vivo* pharmacokinetic studies have shown that the use of an appropriate length of PEG allows one to balance the solubility, intestinal absorption, and hepatic metabolism to obtain either systemic (**P9**) or gut-restricted TGR5 agonists (**P11** and **P12**).

Through this process, **P11** (n = 31−57) was identified as a potent agonist (mTGR5 EC_{50} = 25 nM) with high intestinal exposure combined to extremely low passive membrane crossing. **P11** was selected to assess the feasability of apical stimulation of GLP-1 secretion *in vivo*. As maximal GLP-1 secretion is expected when TGR5 is activated in distal sections of the gut and in line with the pharmacokinetics observed in the intestine for **P11**, GLP-1 secretion was measured 8 h after oral dosing of **P11**. Although **P11** reached a millimolar concentration (>10,000*EC_{50}) in the lumen of TGR5 expressing sections of the intestine, it only weakly triggered GLP-1 secretion. It was reported in the literature that functional TGR5 is mostly located on the basolateral side of enteroendocrine L cells and that crossing the intestinal epithelium is required before bile acids or non steroidal TGR5 agonists can trigger a GLP-1 secretory response.[26] The weak GLP-1 secretion observed with the luminally restricted agonist **P11**, combined with our previous observation that a gut-targeted but membrane-permeant TGR5 agonist of the same family[21] actually triggers GLP-1 secretion after oral administration, is consistent with a previous work showing that TGR5 agonists trigger the GLP-1 secretory response predominantly by reaching the basolateral side of the L cells embeded in the intestinal epithelium.[26]

CONCLUSIONS

Many aspects described in this work are relevant for drug research programs focusing on organ-targeted drugs that require an optimization approach different from the classical route. Our study indeed demonstrates that increasing chain length in a series of PEGylated compounds expectedly increases the aqueous solubility of small organic scaffolds and decreases their susceptibility to oxidative metabolism and their passive permeation through cell membranes. Surprisingly, PEGylation does not preclude interactions with efflux pumps, at least for chains smaller than $n \leq 36$.

The study of the PK profile of several PEGylated compounds provides a general knowledge and guidelines for the design of topical intestinal compounds that could be transposable to modulators of other intestinal targets. It also could be very useful to design molecules for oral or parenteral routes, with fine-tuned interactions with cell membranes and efflux pumps, thereby controlling organ distribution in general and brain exposure in particular.

EXPERIMENTAL SECTION

***In Vitro* TGR5 Assay.** TGR5 activation by compounds and subsequent increase in intracellular cAMP were evaluated using a luciferase reporter gene assay. Human embryonic kidney (HEK) 293 cells were transiently co-transfected with pCMV tag4b-TGR5h (to determine hTGR5 activation) or pCMV AC6-TGR5m (to determine mTGR5 activation) expression plasmids and the pCRE TA-Luciferase reporter plasmid using the JET PEI reagent (Polyplus transfection). Transfected cells were seeded in 96-well plates and incubated overnight with the compounds at increasing concentrations in duplicate. Lithocholic acid (LCA) at 10 μM was used as a positive reference compound. The cAMP-dependent luciferase expression was followed using the BrightGlo reagent according to the manufacturer (Promega) instructions. Luminescence was measured with a Mithras plate reader (Berthold). Data were expressed as the percentage of the 10 μM LCA value, and EC_{50} values were calculated using XL fit 5 software or GraphPad Prism 5. Concentration−response curves were

https://dx.doi.org/10.1021/acs.jmedchem.0c01774
J. Med. Chem. 2021, 64, 1593−1610

fitted by a nonlinear regression analysis to a four-parameter logistic equation.

LC-MS/MS ADME Methods. Chromatography was performed using a UPLC system, an Acquity I-Class (Waters). Separation was achieved on a Waters Acquity BEH C18 column (2.1 mm × 50 mm, 1.7 μm). The autosampler and column oven temperatures were 10 and 40 °C, respectively, and the sample injection volume was 1 μL. The mobile phase consisted of 0.1% formic acid in water as solvent A and 0.1% formic acid in acetonitrile as solvent B at a flow rate of 600 μL/min. The gradient was as follows: 0−0.2 min (98%A and 2%B), 2−2.5 min (2%A and 98%B), 2.6 min (98%A and 2%B), 4 min (98% A and 2%B). The gradient step was linear. Mass spectrometry was performed using a Xevo TQD (Waters Corporation) mass spectrometer. The detection of analytes was achieved by electrospray ionization (ESI) in the positive mode with the appropriate MRM transition. For polydisperse PEGylated compounds, LC-MS analyses were performed using several transitions of several of the most abundant species in the mixture. Other mass spectrometer settings were as follows: capillary voltage and cone voltage were optimized for each compound, desolvation temperature 600 °C at a gas flow of 1200 L/h and cone gas flow 50 L/h. The LC-MS/MS instrument was controlled by MassLynx software (Waters).

Solubility Measurements. *Method A.* Ten microliters of a 10 mM solution in DMSO of the compound was diluted either in 490 μL of PBS pH 7.4 or in organic solvent MeOH in a PP tube (n = 3 for PBS, n = 6 for methanol). The tubes were gently shaken for 24 h at room temperature. Then, PBS tubes and three of the six methanol tubes were centrifuged for 5 min at 4000 rpm and filtered over 0.45 μm filters (Millex-LH Millipore). Then, 10 μL of each sample was diluted in 490 μL of MeOH before LC-MS analysis. The solubility is determined by the ratio of mass signal area PBS/organic solvent.

Method B. Water was added to a known amount of the solid compound to reach the tested concentration. After 24 h of mixing, the solution was centrifuged and the supernatant was diluted in methanol before LC-MS analysis. The compound is quantified against a methanol calibration curve.

LogD Measurements. Forty microliters of a 10 mM solution in DMSO of the compound was diluted in 1.960 mL of a 1/1 octanol/PBS at pH 7.4 mixture. The mixture was gently shaken for 2 h at room temperature. Ten microliters of each phase was diluted in 490 μL of MeOH and analyzed by LC-MS/MS. Each compound was tested in triplicate. LogD was determined as the logarithm of the ratio of concentration of product in octanol and PBS, respectively, determined by mass signals.

Microsomal Stability. Male mouse (CD-1) liver microsomes (BD Gentest) were used. All incubations were performed in duplicate in a shaking water bath at 37 °C. The incubation mixtures contained 1 μM compound with 1% methanol used as a vehicle, mouse liver microsomes (0.3 mg of microsomal protein per mL), 5 mM $MgCl_2$, 1 mM NADP, 5 mM glucose 6-phosphate, 0.4 U mL^{-1} glucose 6-phosphate dehydrogenase, and 50 mM potassium phosphate buffer (pH 7.4) in a final volume of 0.5 mL. Aliquots were removed at 5, 10, 20, 30, and 40 min after microsome addition, and the reaction was stopped by adding four volumes of ice-cold acetonitrile containing a 200 nM internal standard. The samples were centrifuged for 10 min at 10,000 rpm and, the supernatants were transferred in matrix tubes for LC-MS/MS analysis. Each compound was quantified by converting the corresponding analyte/internal standard peak area ratios to percentage drug remaining, using the initial ratio values in control incubations as 100%. Propranolol, known as a high hepatic clearance drug in rodents, was used as a quality-control compound for the microsomal incubations. *In vitro* intrinsic clearance (CLint expressed as μl/min/mg) was calculated according to the following formula: CLint = dose/AUC_∞, where dose is the initial amount of drug in the incubation mixture (1 μM) and AUC_∞ is the area under the concentration versus time curve extrapolated to infinity. The slope of the linear regression from log percentage remaining versus incubation time relationships ($-k$) was used in the conversion to *in vitro* $t_{1/2}$ values by: $t_{1/2} = -\ln(2)/k$.

Caco-2 Permeation Assay. Caco-2 cells (0.4×10^5, ATCC no. HTB-37), at passage 28, were seeded on a 25 cm^2 plastic flask and changed every 2 days with complete medium containing high glucose Dulbecco's modified Eagle's medium (DMEM) with L-glutamine supplemented by 10% of fetal calf/bovine serum, 1% of non-essential amino acids without L-glutamine. The paracellular barrier characteristics of the Caco-2 cells monolayer were monitored using measurement of the permeability to the non-permeant fluorescent molecule, Lucifer Yellow (LY). Caco-2 cells were trypsinized after 3 days of incubation while they cover 80−90% of the flask and seeded at a density of 5×10^5 in 75 cm^2 flasks in complete medium After 5−6 days, Caco-2 cells reach a high cell density (>0.5×10^5 cells/cm^2) and are then passaged into cell HTS 24-well plates with 0.4 μm polycarbonate membrane inserts. Cells were seeded at 200,000 cells/cm^2 and cultivated for 21 days in complete medium. Media was replaced every 2 days. Compound solutions were prepared in HEPES-buffered Ringer's (RH) solution (NaCl 150 mM, KCl 5.2 mM, $CaCl_2$ 2.2 mM, $MgCl_2$ 0.2 mM, $NaHCO_3$ 6 mM, glucose 2.8 mM, HEPES 5 mM, water for injection), pH = 7.4, at a final concentration of 5 or 10 μM for tested drugs. For the A → B transport experiment, 0.2 mL of the compound solution was placed on the apical side of the cells and samples were taken from the basolateral compartment. For the B → A transport experiment, 0.8 mL of the solution was placed on the basolateral side of the cells and samples were taken from the apical side. Transport studies were done in Transwell polycarbonate: HTS 24-well plate inserts (surface area: 0.33 cm^2 to 0.4 μm pore size). Cells were equilibrated for 10 min in transport buffer prior to the transport experiment, and then incubations with compounds were performed at 37 °C under agitation. After 1 h, aliquots were taken from each compartment and sampled in 96-well plates with glass insert. Samples were analyzed by LC−MS/MS analysis. Permeation are calculated using the formulas below:

$$P_{appA\to B} = \frac{V_{receiver} \times \text{area } BL_{t=x}}{\text{time} \times \text{surface membrane} \times \text{area } AL_{t=0}}$$

$$P_{appB\to A} = \frac{V_{receiver} \times \text{area } A_{t=x}}{\text{time} \times \text{surface membrane} \times \text{area } BL_{t=0}}$$

BBB Permeation. To reproduce *in vitro* the human BBB, human umbilical cord blood is collected. Infants' parents signed an informed consent form, in compliance with the French legislation. The protocol was approved by the French Ministry of Higher Education and Research (CODECOH Number DC2011-1321). All experiments were carried out in accordance with the approved protocol. Briefly, hematopoietic stem cells were isolated from the umibilical coord blood and cells were differentiated into endothelial cells as previously described.[27] Then, endothelial cells are seeded on Transwell Costar polycarbonate inserts, 0.4 μm pore size, coated with Matrigel matrix (Corning), and co-cultured with brain pericytes for 6 days. After this period, endothelial cells display the major features of the blood−brain barrier observed *in vivo* and are then named brain-like endothelial cells (BLECs).[28−30] Toxicity and drug transport of tested compounds were evaluated in HEPES-buffered Ringer's solution at 10 μM. The culture medium was removed and replaced with test drugs (with 1 μM sodium fluorescein used as an integrity control) in the donor compartment. After 60 min, aliquots were taken in abluminal and luminal compartments of the cell culture. Samples were analyzed by LC-MS/MS analysis.

Endothelial permeability coefficient (Pe) is calculated as described previously.[31]

In this calculation method, both filter without cell permeability (PSf = insert filter + matrigel coating) and filter plus cell permeability (PSt = filter + matrigel + ECs) are taken into account according to the formula: 1/PSe = 1/PSt + 1/PSf, where PS is the permeability × surface area product (in microliters per minute) obtained by dividing the volume cleared from the donor to the receiver compartment (in μL) by the duration of the experiment (60 min).

The PSe values are divided by the surface area of the filter (1.2 cm^2) to generate the endothelial permeability coefficient (Pe) in centimeters per minute.

https://dx.doi.org/10.1021/acs.jmedchem.0c01774
J. Med. Chem. 2021, 64, 1593−1610

Caco-2 Pump Out Assay. This assay was assessed as previously described.[25] Briefly, Caco-2 cells were seeded at 100,000 cells/cm^2 (20,000 cells/well) into Collagen type I 96-well plates and cultivated in complete medium. Media was replaced every 2 days. After a culture period of 6 days, Caco-2 cells in 96-well plates were washed one time in with RH solution and incubated for 120 min with 10 μM rhodamine 123 (Rho 123) or for 15 min with 5 μM 5-chloromethylfluorescein diacetate (CMFDA).

After an incubation period, Caco-2 cells were washed two times with RH buffer and incubated with or without test compounds. The clearance of the fluorescent dyes from Caco-2 cells (Kout) were monitored by fluorescence measurement (λex = 501 nm and λem = 538 nm for R123 and λex = 485 nm and λem = 538 nm for CMFDA) using a microplate fluorimeter (BioTek, H1, Vermont, Winooski). The amount of dye expelled from the cells was measured every 2 min over 1 h at 37 °C. The Kout of the dyes in presence or absence of test compounds (in RFU/min) were calculated as the slope of the curve of the cumulative amount of dye over time (Kout = $\frac{\Delta \mathrm{RFU}}{\Delta t}$).

***In Vivo* Experiments.** *Animals and Diets.* Ten to 12 week-old male C57Bl6 mice were purchased from Charles River (France) and fed ad libitum with a standard diet (UAR A04, Villemoison/Orge, France). All animals were maintained in standard animal cages under conventional laboratory conditions (12 h/12 h light/dark cycle, 22 °C) with ad libitum access to food and water. The animals were maintained in compliance with European standards for the care and use of laboratory animals and experimental protocols approved by the local Animal Ethical Committee (agreement no. 01134.03).

Pharmacokinetics. Compounds were dissolved in distilled water/0.1% Tween and administered orally at 32 μmol/kg to 8 week-old, male, C57Bl6 mice (approximately 25−30 g) (Charles River). Compounds were administered to overnight fasted animals. Three mice per time point were anesthetized with isoflurane, and aliquots taken from the retro-orbital sinus using sampling heparinated tubes (4 °C) at 10 min, 20 min, 30 min, 1 h, 2 h, and 4 h after administration of a single dose of compounds. The blood samples were centrifuged (5000*g*, 15 min) for plasma separation and stored at −80 °C before compound measurement. Plasma samples were thawed on ice. Aliquots were precipitated with ice-cold acetonitrile (:10 ratio) containing compound **3** (0.2 μM) as an internal standard. The samples were vigorously mixed with a vortex and centrifuged for 10 min at 10,000 rpm, 4 °C, and the supernatants were transferred into Matrix tubes for LC-MS/MS analysis. Spiked standard solutions (1, 3, 10, 30, 100, 300, 1000, 3000, 10,000, and 30,000 nM) were prepared the same way. After rodent sacrifice, gallbladders, livers, and intestines were removed. Gallbladders were immediately measured using a vernier caliper. Intestines were cut to isolate the duodenum, jejunum, ileum, and colon. All tissues were frozen in liquid nitrogen and stored at −80 °C. Compounds in tissues were extracted with a MeOH/CH_3CN 50:50 mixture (using a vortex for feces or a Tissue Lyzer II from Qiagen for tissues). After centrifugation (10,000 rpm, 10 min, 4 °C) of the homogenate samples, supernatants were diluted (1 to 10) with ice-cold acetonitrile containing compound **3** (0.2 μM) as an internal standard. After the last centrifugation, the supernatants were transferred into Matrix tubes for LC-MS/MS analysis.

Synthetic Materials and Methods. All commercial reagents and solvents were used without further purification. Microwave-assisted chemical reactions were conducted on a CEM Discover synthesis system or a Biotage Initiator+ microwave synthesizer. Flash column chromatography was performed on prepacked columns (Grace Resolv flash cartridges, Grace). Preparative HPLC were performed using a Varian ProStar system using an Omnisphere 10 C_{18} column (250 mm × 41.4 mm) Dynamax from Varian, Inc. or a Waters-2 system using a XBridge Prep C18 5 μm OBD (50 mm × 250 mm). A gradient starting from 10 %CH_3CN/90% H_2O/ 0.1% formic acid and reaching 100%CH_3CN/0.1% formic acid at a flow rate of 80 mL/minutes was used on the Varian ProStar system. Products were detected by UV absorption at 215 nm and/or 254 nm. A gradient mixture of CH_3CN and water in ammonium formate buffer at pH 9.2 or pH 3.8 and a flow rate at 80 mL/min was used on Waters-2 system. Products were detected by UV absorption and/or by MS. NMR spectra were recorded on a Bruker DRX-300 spectrometer. Chemical shifts are in parts per million (ppm). The assignments were made using one-dimensional (1D) ^{1}H and ^{13}C spectra and two-dimensional (2D) HSQC, HMBC and COSY spectra. LCMS analysis was performed on a Waters Alliance Micromass ZQ 2000, using an XBridge C18 column (3.5 μm particle size, dimensions 50 mm × 4.6 mm). A mixture of water and acetonitrile was used as mobile phase in gradient elution. pH of mobile phase was adjusted with HCOOH and NH_4OH to form a buffer solution at pH 3.8. The analysis time is 5 min (at a flow rate at 2 mL/min). Purity (%) was determined by reversed-phase HPLC, using UV detection (215 nm), and all compound showed purity greater than 95%. Purification yields were not optimized. Final compounds were isolated as amorphous solids without collection of melting point data.

General Procedure A. In a round-bottom flask were added the isothioureido derivative (1 eq), potassium carbonate (1 eq), sodium iodide (0.5 eq), and acetonitrile (QS 0.2 M). The suspension was stirred at room temperature for 10 min, and benzyl halide (1 eq) was then added. The suspension was stirred at room temperature overnight. The reaction mixture was then evaporated; the residue was dissolved in EtOAc and washed with water and brine. The organic phase was dried over Na_2SO_4 and evaporated. The residue was purified by flash chromatography using as an eluent a mixture of cyclohexane/EtOAc.

General Procedure B. In a round-bottom flask were introduced the isothioureido-acetamide derivative (1 eq), ethyl acetate (QS 0.1 M), diisopropylethylamine (6 eq), and T_3P (3 eq). The reaction mixture was heated at reflux for 24 h. Diisopropylethylamine and T_3P were added until completion. The reaction mixture was then diluted in EtOAc and washed with a saturated aqueous solution of $NaHCO_3$ and brine. The organic phase was dried over Na_2SO_4 and evaporated to dryness. The residue was purified by flash chromatography using as an eluent a mixture of cyclohexane/EtOAc.

General Procedure C. In a microwave tube were introduced the isothioureido-acetamide derivative (1 eq), ethyl acetate (QS 0.1 M), diisopropylethylamine (6 eq), and T3P (3 eq). The reaction mixture was heated under microwave irradiation at 150 °C for 10 min. The reaction mixture was then diluted with EtOAc and washed with a saturated aqueous solution of $NaHCO_3$ and brine. The organic phase was then dried over Na_2SO_4 and evaporated. The residue was purified by flash chromatography using as an eluent a mixture of cyclohexane/EtOAc.

General Procedure D. In a microwave tubes were added 5-amino-2-thio-imidazole derivative (1 eq), phenylboronic derivative (1 eq), cesium carbonate (1.75 eq), and $Pd(Ph_3P)_4$ (0.175 eq). A mixture of 222 μL of water (QS 0.8 M), 594 μL of dimethoxyethane (QS 0.3 M), and 89.1 μL of ethanol (QS 0.5 M) was prepared and poured into the microwave tube. The reaction mixture was heated under microwave irradiation at 100 °C for 10 min. The reaction mixture was then evaporated to dryness, diluted in ethyl acetate, filtered on Celite, washed with water and brine, dried over $MgSO_4$, and evaporated to dryness.

General Procedure E. In a round-bottom flask were introduced 3,5-difluoro-4-(hydroxymethyl)phenol (1.2 eq), methylbenzenesulfonic acid polyethyleneglycol ester derivatives (1 eq), potassium carbonate (1.2 eq), and acetonitrile (QS 0.3 M). The suspension was stirred under reflux overnight. The reaction mixture was then filtrated and evaporated. The residue was purified by flash chromatography using as an eluent a mixture of DCM/MeOH.

General Procedure F. In a round-bottom flask were introduced [2,3-difluoro-4-(methoxypolyethyleneglycoxy)phenyl]methanol derivatives (1 eq), triethylamine (1.5 eq), and dry DCM (QS 0.4 M) at 0 °C. Mesyl chloride (1.2 eq) was then added in the reaction mixture dropwise, and it was stirred at room temperature overnight. After several hours, triethylamine and mesylchloride could be added several times until completion. The reaction mixture was evaporated to dryness.

*(3,4-Dimethoxyphenyl)methylamine (**1a**).* In a 250 mL flask were added 3,4-dimethoxyaniline (3 g, 19.58 mmol) and sodium methoxide

https://dx.doi.org/10.1021/acs.jmedchem.0c01774
J. Med. Chem. 2021, 64, 1593−1610

(5.29 g, 97.92 mmol) in 35 mL of dry methanol. Then, paraformaldehyde (1.18 g, 39.17 mmol) and 15 mL of dry methanol were added. Molecular sieve (4 Å) was then added, and the mixture was stirred overnight at room temperature. Sodium borohydride (0.74 g, 19.58 mmol) was then added, and the mixture was heated under reflux for 1 h. The mixture was then evaporated and dissolved in EtOAc and water, and the two phases were separated. The aqueous phase was then basified by addition of a saturated aqueous solution of $NaHCO_3$ and extracted by EtOAc. The organic phases were washed with a saturated aqueous solution of $NaHCO_3$ and brine, dried over Na_2SO_4, and evaporated to dryness to give the titled product as an oily residue (2.67 g, 77%). It was used without further purification in the next step of the synthesis. LC-MS: t_R = 2.12 min. MS $[M + H]^+$ m/z = 168.0. ^{1}H NMR (300 MHz, DMSO-d_6): δ (ppm) 2.62 (d, J = 5.0 Hz, 3H), 3.61 (s, 3H), 3.69 (s, 3H), 5.20 (q, J = 4.9 Hz, 1H), 5.99 (dd, J = 8.5, 2.5 Hz, 1H), 6.22 (d, J = 2.5 Hz, 1H), 6.71 (d, J = 8.5 Hz, 1H).

*[2-(3,4-Dimethoxy-N-methylanilino)-2-oxoethyl]ammonium Formate (**1b**).* In a 250 mL flask were introduced a solution of 2.67 g of (3,4-dimethoxyphenyl)methylamine (**1a**) and 7.9 mL of DIEA in 45 mL of DCM (dried over Na_2SO_4). The solution was stirred at 0 °C. Then, a solution of 2.4 mL of chloroacetyl chloride in 30 mL of DCM (dried over Na_2SO_4) was added dropwise in the flask. The mixture was then evaporated to dryness to give a brown residue, which was used without further purification in the next step of the synthesis. The residue corresponding to 2-chloro-*N*-(3,4-dimethoxyphenyl)-*N*-methylacetamide was dissolved in 25 mL of ethanol 95% and added dropwise in a 500 mL flask containing 320 mL of aqueous ammonia at 65 °C. The reaction mixture was then evaporated to dryness. The residue was dissolved in DCM and extracted several times with an aqueous solution of HCOOH 1 M. The aqueous phase was then evaporated to dryness, and the residue was triturated in acetonitrile. The supernatant was evaporated to dryness to give the titled product as a brown powder (3.82 g, 75% yield over two steps). MS $[M + H]^+$ m/z = 225.1. ^{1}H NMR (300 MHz, DMSO-d_6): δ (ppm) 3.17 (s, 3H), 3.76−3.77 (m, 6H), 3.99 (s, 2H), 6.90 (dd, J = 8.4, 2.2 Hz, 1H), 6.99−7.03 (m, 2H), 8.00 (brs, 3H), 8.20 (s, 1H).

*[2-(3,4-Dimethoxy-N-methylanilino)-2-oxoethyl]ammonium 2,2,2-Trifluoroacetate (**1c**).* In a 250 mL flask was added (3,4-dimethoxyphenyl)methylamine (**1a**) (903 mg, 5.41 mmol) in 4 mL of EtOAc. Then, 2-(*tert*-butoxycarbonylamino)acetic acid (1136 mg, 6.49 mmol), T3P (4.78 mL, 8.12 mmol), and DIEA (2.83 mL, 16.21 mmol) were added. The mixture was stirred at room temperature for 30 min. Then, the reaction mixture was diluted with EtOAc and washed with water and a saturated aqueous solution of $NaHCO_3$ and brine. The organic phase was dried over $MgSO_4$ and evaporated to dryness to give the *tert*-butyl *N*-[2-(3,4-dimethoxy-*N*-methylanilino)-2-oxoethyl]carbamate as a reddish powder (1.77 g, 100%). LC-MS: t_R = 2.35 min. MS: $[M + H]^+$ m/z = 325.0. ^{1}H NMR (300 MHz, $CDCl_3$): δ (ppm) 1.42 (s, 9H), 3.27 (s, 3H), 3.68 (s, 2H), 3.89 (m, 6H), 6.68 (d, J = 2.4 Hz, 1H), 6.76 (dd, J = 8.4, 2.4 Hz, 1H), 6.86 (d, J = 8.5 Hz, 1H).

In a 50 mL flask, *tert*-butyl *N*-[2-(3,4-dimethoxy-*N*-methylanilino)-2-oxoethyl]carbamate (1770 mg, 5.46 mmol) was dissolved in 13.6 mL of DCM. TFA (5.53 mL, 72.21 mmol) was added, and the reaction mixture was stirred at room temperature for 30 min. The reaction mixture was evaporated to dryness to give a purple oil, corresponding to the expected product (1.85 g, 100%). The residue was used without further purification in the next step of the synthesis. MS $[M + H]^+$ m/z = 225.1.

*N-(3,4-Dimethoxyphenyl)-2-[3-(4-fluorophenyl)iisothioureido]-N-methylacetamide (**1d**).* 4-Fluorophenylisothiocyanate (1.51 g, 9.83 mmol) and TEA (1.59 mL, 11.79 mmol) were added in a 250 mL flask in 15 mL of ethanol. [2-(3,4-Dimethoxy-*N*-methylanilino)-2-oxoethyl]ammonium formate (3.2 g, 9.83 mmol) (**1b**) were dissolved in 115 mL of ethanol, TEA (1.33 mL, 9.83 mmol) were added, and the mixture was added dropwise at room temperature. After the addition, the reaction was over. The reaction mixture was evaporated to dryness and purified by flash chromatography using as an eluent a mixture of cyclohexane/EtOAc to give the titled product as a yellowish powder (2.8 g, 76%). LC-MS: t_R = 2.83 min. MS $[M - H]^-$ m/z = 244.1. ^{1}H NMR (300 MHz, DMSO-d_6): δ (ppm) 2.49 (s, 3H), 3.78 (m, 6H), 4.00 (d, J = 4.1 Hz, 2H), 6.92 (dd, J = 8.4, 1.8 Hz, 1H), 7.01−7.03 (m, 2H), 7.15 (m, 2H), 7.45 (m, 2H), 7.73 (m, 1H), 9.90 (s, 1H).

*2-[2-(2,6-Difluorobenzyl)-3-(4-fluorophenyl)isothioureido]-N-(3,4-dimethoxyphenyl)-N-methylacetamide (**1e**).* The titled product was obtained without purification as an oily residue (1.15 g, 91%), following Procedure A, using *N*-(3,4-dimethoxyphenyl)-2-[3-(4-fluorophenyl)isothioureido]-*N*-methylacetamide (**1d**) (940 mg) and 2-bromomethyl-1,3-difluorobenzene (518 mg). MS $[M + H]^+$ m/z = 504.0. ^{1}H NMR (300 MHz, DMSO-d_6): δ (ppm) 3.16 (s, 3H), 3.69−3.76 (m, 8H), 4.19 (s, 2H), 6.61 (m, 2H), 6.79−6.89 (m, 2H), 6.95−7.00 (m, 4H), 7.05−7.13 (m, 3H), 7.38 (m, 1H).

*[2-(2,6-Difluorobenzylsulfanyl)-3-(4-fluorophenyl)-3H-imidazol-4-yl]-(3,4-dimethoxyphenyl)methylamine (**1**).* In a 50 mL flask were added 2-[2-(2,6-difluorobenzyl)-3-(4-fluorophenyl)isothioureido]-*N*-(3,4-dimethoxyphenyl)-*N*-methylacetamide (**1e**) (500 mg), 10 mL of EtOAc, NEt_3 (843 μL), and T3P (1.77 mL). The reaction mixture was then stirred at reflux for 28 h. After 8 h, NEt_3 (843 μL) and T3P (1.77 mL) were added. After 25 h, NEt_3 (422 μL) and T3P (885 μL) were added. After dilution with 20 mL of EtOAc, the solution was washed with a saturated aqueous solution of $NaHCO_3$ and brine. The organic phase was dried over Na_2SO_4 and evaporated. The residue was purified by flash chromatography using as an eluent a mixture of DCM/MeOH. The titled product was obtained as an oily residue (160 mg, 33%). LC-MS: t_R = 3.13 min, MS $[M + H]^+$ m/z = 486.3. HRMS found 486.1437; $C_{25}H_{22}F_3N_3O_2S$ requires 486.1463. ^{1}H NMR (300 MHz, $CDCl_3$): δ (ppm) 2.92 (s, 3H), 3.80 (s, 3H), 3.82 (s, 3H), 4.16 (s, 2H), 6.16 (dd, J = 8.7, 2.7 Hz, 1H), 6.30 (d, J = 2.7 Hz, 1H), 6.72 (d, J = 8.7 Hz, 1H), 6.78 (m, 2H), 6.83−6.85 (m, 4H), 6.92 (s, 1H), 7.19 (m, 1H). ^{13}C NMR (75 MHz, $CDCl_3$): δ (ppm) 25.9, 40.1, 55.9, 56.4, 99.9, 105.5, 111.2, 112.4, 113.6 (t, J = 19.3 Hz), 115.9 (d, J = 22.9 Hz), 124.4, 129.1, 129.2, 130.8, 138.1, 139.6, 142.7, 143.2, 149.6, 161.1 (dd, J = 250.0, 7.7 Hz), 162.2 (d, J = 249.0 Hz).

*N-(3,4-Dimethoxyphenyl)-2-[3-(4-fluoro-3-methoxyphenyl)-isothioureido]-N-methylacetamide (**2d**).* In a 25 mL flask, TCDI (133 mg, 0.749 mmol) was dissolved in 3 mL of dioxane. [2-(3,4-Dimethoxy-*N*-methylanilino)-2-oxoethyl]ammonium 2,2,2-trifluoroacetate (**1c**) (230 mg, 0.681 mmol) in 3.50 mL of dioxane was then added dropwise. The solution was then stirred at room temperature for 1.5 h. 4-Fluoro-3-methoxyaniline (106 mg, 0.750 mmol) and NEt_3 (285 μL, 2.04 mmol) were added to the solution. The reaction mixture was stirred at 60 °C overnight. The solvent was then removed. The residue was dissolved in EtOAc and washed with water, with an aqueous HCl 0.1 N solution, and dried over $MgSO_4$. After evaporation, the residue was purified by flash chromatography using as an eluent a mixture of cyclohexane/EtOAc (8/2) to give the titled product as an orange solid (136 mg, 49%). LC-MS: t_R = 2.53 min. MS $[M + H]^+$ m/z = 408.1. ^{1}H NMR (300 MHz, DMSO-d_6): δ (ppm) 3.16 (s, 3H), 3.74−3.82 (m, 9H), 4.00 (d, J = 4.2 Hz, 2H), 6.84−6.96 (m, 2H), 6.98−7.06 (m, 2H), 7.15 (dd, J = 11.3, 8.7 Hz, 1H), 7.37 (dd, J = 7.9, 2.2 Hz, 1H), 7.77 (brs, 1H), 9.91 (s, 1H).

*2-[2-(2,6-Difluorobenzyl)-3-(4-fluoro-3-methoxyphenyl)-isothioureido]-N-(3,4-dimethoxyphenyl)-N-methylacetamide (**2e**).* The titled product was obtained as a yellowish oil (156 mg, 91%) without purification, following Procedure A, using *N*-(3,4-dimethoxyphenyl)-2-[3-(4-fluoro-3-methoxyphenyl)isothioureido]-*N*-methylacetamide (**2d**) (124 mg, 304 μmol) and 2-bromomethyl-1,3-difluorobenzene (63 mg, 304 μmol). LC-MS: t_R = 3.29 min. MS $[M + H]^+$ m/z = 534.2. ^{1}H NMR (300 MHz, $CDCl_3$): δ (ppm) 3.28 (s, 3H), 3.78−3.84 (m, 11H), 4.11 (brs, 2H), 5.82 (s, 1H), 6.29 (brs, 1H), 6.44 (d, J = 6.3 Hz, 1H), 6.61−6.89 (m 6H), 7.13−7.26 (m, 1H).

*[2-(2,6-Difluorobenzylsulfanyl)-3-(4-fluoro-3-methoxyphenyl)-3H-imidazol-4-yl]-(3,4-dimethoxyphenyl)methylamine (**2**).* The titled product was obtained as an orange powder (143 mg, 63%), following Procedure C, using 2-[2-(2,6-difluorobenzyl)-3-(4-fluoro-3-methoxyphenyl)isothioureido]-*N*-(3,4-dimethoxyphenyl)-*N*-methylacetamide (**2e**) (156 mg, 278 μmol). LC-MS: t_R = 3.42 min. MS [M +

https://dx.doi.org/10.1021/acs.jmedchem.0c01774
J. Med. Chem. 2021, 64, 1593−1610

H]$^+$ m/z = 516.2. ^{1}H NMR (300 MHz, $CDCl_3$): δ (ppm) 2.90 (s, 3H), 3.54 (s, 3H), 3.82 (s, 6H), 4.20 (s, 2H), 6.18 (dd, J = 8.7, 2.8 Hz, 1H), 6.33 (d, J = 2.8 Hz, 1H), 6.54 (dd, J = 7.5, 2.4 Hz, 1H), 6.59−6.64 (m, 1H), 6.75 (d, J = 8.7 Hz, 1H), 6.78−6.86 (m, 2H), 6.98 (dd, J = 10.8, 8.6 Hz, 1H), 7.06 (s, 1H), 7.14−7.24 (m, 1H). ^{13}C NMR (75 MHz, $CDCl_3$): δ (ppm) 25.7, 39.9, 55.9, 56.0, 56.6, 99.7, 105.2, 111.1−111.4 (m), 112.6, 112.7 (d, J = 2.4 Hz), 113.6 (t, J = 19.4 Hz), 115.9 (d, J = 19.6 Hz), 119.7 (d, J = 7.3 Hz), 124.9, 129.2 (t, J = 10.2 Hz), 130.9 (d, J = 3.6 Hz), 138.6, 139.0, 142.6, 143.5, 147.5 (d, J = 11.6 Hz), 149.8, 152.0 (d, J = 248.9 Hz), 161.2 (dd, J = 249.9, 7.7 Hz).

*[2,6-Difluoro-4-(methoxypolyethyleneglycoxy)phenyl]methanol (**P3i**) (Average MW = 627 g/mol).* In a round-bottom flask were added methoxypolyethyleneglycol (average MW = 500 g/mol) (1500 mg, 3 mmol) in dry THF (10 mL). The solution was cooled at 0 °C. NaH (107.99 mg, 4.5 mmol) was added, and the reaction mixture was stirred at 0 °C to room temperature for 2 h. Then, 4-methylbenzenesulfonyl chloride (1143.9 mg, 6 mmol) was added at 0 °C, and the reaction mixture was stirred at room temperature for 24 h. The reaction mixture was then evaporated, and the residue was purified by flash chromatography using as an eluent a mixture of DCM/MeOH (94/6) to give a colorless oil corresponding to the expected 2-(*p*-tolylsulfonyloxy)polyethyleglycoxyl 4-methylbenzenesulfonate (1.68 g, 86%). LC-MS: t_R = 2.82 min. MS [M + H_3O]$^+$ m/z = 644.3 (n = 10). ^{1}H NMR (300 MHz, DMSO-d_6): δ (ppm) 2.41 (s, 3H), 3.23 (s, 3H), 3.44−3.49 (m, 36H), 3.57 (m, 2H), 4.10 (m, 2H), 7.48 (d, J = 8.0 Hz, 2H), 7.78 (d, J = 8.3 Hz, 2H). The titled product **P3i** was then obtained as a colorless oil (676 mg, 70%), following Procedure E, using 2-(*p*-tolylsulfonyloxy)polyethyleglycoxyl 4-methylbenzenesulfonate (981 mg, 1.5 mmol) and 3,5-difluoro-4-(hydroxymethyl)phenol (288 mg, 1.8 mmol). LC-MS: t_R = 2.58 min. MS [M + H_3O]$^+$ m/z = 632.2 (n = 10). ^{1}H NMR (300 MHz, DMSO-d_6): δ (ppm) 3.23 (s, 3H), 3.41−3.56 (m, 42H), 3.72 (m, 2H), 4.11 (m, 2H), 4.40 (d, J = 5.5 Hz, 2H), 5.08 (t, J = 5.5 Hz, 1H), 6.71 (m, 2H).

*2-(Chloromethyl)-1,3-difluoro-5-(2-methoxypolyethyleneglycoxy]benzene (**P3ii**) (Average MW = 646 g/mol).* The titled product was obtained without purification (694 mg, 100%), following Procedure F, using [2,6-difluoro-4-(methoxypolyethyleneglycoxy)phenyl]methanol **P3i** (676 mg). LC-MS: t_R = 3.00 min. MS [M + H_3O]$^+$ m/z = 650.2 (n = 10).

*2-[2-[2,6-Difluoro-4-(methoxypolyethyleneglycoxy)benzyl]-3-(4-fluorophenyl)isothioureido]-N-(3,4-dimethoxyphenyl)-N-methylacetamide (**P3a**) (Average MW = 1012.7 g/mol).* The titled product was obtained as a brown oil (499 mg, 47%), following Procedure A, using 2-(chloromethyl)-1,3-difluoro-5-(2-methoxypolyethyleneglycoxy]benzene **P3ii** (694 mg, 1.05 mmol) and *N*-(3,4-dimethoxyphenyl)-2-[3-(4-fluorophenyl)isothioureido]-*N*-methylacetamide (**1d**) (397 mg, 1.05 mmol). LC-MS: t_R = 3.12 min. MS [M + H + H_3O]$^{2+}$ m/z = 518.4 (n = 10). ^{1}H NMR (300 MHz, DMSO-d_6): δ (ppm) 3.16 (s, 3H), 3.22 (s, 3H), 3.14−3.55 (m, 40H), 3.69−3.76 (m, 8H), 4.10 (s, 2H), 6.60−7.01 (m, 9H).

*[2-[2,6-Difluoro-4-(2-methoxypolyethyleneglycoxy)-benzylsulfanyl]-3-(4-fluorophenyl)-3H-imidazol-4-yl]-(3,4-dimethoxyphenyl)methylamine (**P3**) (Average MW = 972.1 g/mol, n = 9−13).* The titled compound was obtained after purification by preparative HPLC as an orange oil (131 mg, 27%), following Procedure B, using 2-[2-[2,6-difluoro-4-(methoxypolyethyleneglycoxy)benzyl]-3-(4-fluorophenyl)-isothioureido]-*N*-(3,4-dimethoxyphenyl)-*N*-methylacetamide (**P3a**) (499 mg, 493 μmol). LC-MS: t_R = 3.12 min. MS [M + H + H_3O]$^{2+}$ m/z = 487.2 (n = 10). ^{1}H NMR (300 MHz, DMSO-d_6): δ (ppm) 2.92 (s, 3H), 3.23 (s, 3H), 3.42−3.55 (m, 42H), 3.63−3.64 (m, 6H), 3.70−3.73 (m, 2H), 3.99 (s, 2H), 4.09−4.12 (m, 2H), 6.06 (dd, J = 8.6, 2.7 Hz, 1H), 6.21 (d, J = 2.7 Hz, 1H), 6.67−6.70 (m, 2H), 6.75 (d, J = 8.8 Hz, 1H), 6.96 (s, 1H), 7.09−7.22 (m, 4H). ^{13}C NMR (75 MHz, DMSO-d_6): δ (ppm) 26.1, 55.9, 56.5, 58.5, 68.6, 69.0, 70.0, 70.2, 70.3, 71.7, 99.1 (d, J = 28.0 Hz), 99.9, 105.4, 105.5 (t, J = 20.6 Hz), 113.7, 116.3 (d, J = 22.9 Hz), 124.3, 130.0 (d, J = 9.0 Hz), 131.5 (d, J = 3.6 Hz), 137.3, 140.1; 142.5, 143.4, 149.7, 161.7 (dd, J = 286.1, 11.7 Hz), 162.1 (d, J = 275.7 Hz).

*[2,6-Difluoro-4-(methoxypolyethyleneglycoxy)phenyl]methanol (**P4i**) (Average MW = 947 g/mol).* The titled product was obtained as a white viscous residue after purification by preparative HPLC (697 mg, 61%), following Procedure E, using polyethyeneglycol methyl ether tosylate (average molecular weight = 900 g/mol) (1080 mg, 1.2 mmol) and 3,5-difluoro-4-(hydroxymethyl)phenol (211 mg, 1.32 mmol). LC-MS: t_R = 2.23 min. MS [M + H_3O]$^+$ m/z = 808.2 (m = 14). ^{1}H NMR (300 MHz, DMSO-d_6): δ (ppm) 3.23 (s, 3H), 3.38−3.58 (m, 66H), 3.72 (m, 2H), 4.11 (m, 2H), 4.40 (s, 2H), 6.71 (m, 2H). 1H NMR (DMSO-d_6): δ (ppm) 3.23 (s, 3H), 3.38−3.58 (m, 66H), 3.72 (m, 2H), 4.11 (m, 2H), 4.40 (s, 2H), 6.71 (m, 2H).

*2-(Chloromethyl)-1,3-difluoro-5-(2-methoxypolyethyleneglycoxy]benzene (**P4ii**) (Average MW = 1033 g/mol).* The titled product was obtained (710 mg, 100%), following Procedure F, using [2,6-difluoro-4-(methoxypolyethyleneglycoxy)-phenyl]methanol **P4i** (697 mg, 738 μmol). LC-MS: t_R = 2.73 min. MS [M + $2H_3O$]$^{2+}$ m/z = 488.3 (n = 17).

*2-[2-[2,6-Difluoro-4-(methoxypolyethyleneglycoxy)benzyl]-3-(4-fluorophenyl)isothioureido]-N-(3,4-dimethoxyphenyl)-N-methylacetamide (**P4a**) (Average MW = 1209 g/mol).* The titled product was obtained as a pale pink solid (146 mg, 17%), following Procedure A, using 2-(chloromethyl)-1,3-difluoro-5-(2-methoxypolyethyleneglycoxy]benzene **P4ii** (711 mg, 738 μmol) and *N*-(3,4-dimethoxyphenyl)-2-[3-(4-fluorophenyl)isothioureido]-*N*-methylacetamide (**1d**) (279 mg, 738 μmol). LC-MS: t_R = 2.87 min. MS [M + H + H_3O]$^{2+}$ m/z = 606.3 (n = 15).

*[2-[2,6-Difluoro-4-(2-methoxy-polyethyleneglycoxy)-benzylsulfanyl]-3-(4-fluorophenyl)-3H-imidazol-4-yl]-(3,4-dimethoxyphenyl)methylamine (**P4**) (Average MW = 1204 g/mol, n = 10−22).* The titled compound was obtained after purification by preparative HPLC as an orange oil (20 mg, 13%), following Procedure B, using 2-[2-[2,6-difluoro-4-(methoxypolyethyleneglycoxy)benzyl]-3-(4-fluorophenyl)-isothioureido]-*N*-(3,4-dimethoxyphenyl)-*N*-methylacetamide (**P4a**) (average MW = 1209 g/mol) (148 mg, 122 μmol). LC-MS: t_R = 2.85 min. MS [M + H + H_3O]$^{2+}$ m/z = 619.2 (n = 16). ^{1}H NMR (300 MHz, CD_2Cl_2): δ (ppm) 2.96 (s, 3H), 3.36 (s, 3H), 3.50−3.72 (m, 80H), 3.74−3.77 (m, 6H), 3.78−3.88 (m, 4H), 4.04−4.14 (m, 4H), 6.15 (dd, J = 8.7, 2.8 Hz, 1H), 6.27 (d, J = 2.8 Hz, 1H), 6.41−6.50 (m, 2H), 6.72 (d, J = 8.7 Hz, 1H), 6.96−7.07 (m, 5H). ^{13}C NMR (75 MHz, CD_2Cl_2): δ (ppm) 25.8, 40.1, 55.8, 56.4, 58.6, 68.3, 69.2, 70.3, 70.4, 70.5, 70.8, 71.9, 98.1−98.7 (m), 100.1, 105.5, 105.6 (t, J = 20.5 Hz), 112.9, 115.7 (d, J = 23.0 Hz), 124.0, 129.3 (d, J = 8.8 Hz), 131.1 (d, J = 3.3 Hz), 138.0, 139.8, 142.8, 143.3, 149.8, 159.7 (t, J = 14.5 Hz), 161.6 (dd, J = 247.1, 11.3 Hz), 162.3 (d, J = 248.3 Hz).

*[2,6-Difluoro-4-(methoxypolyethyleneglycoxy)phenyl]methanol (**P5i**) (Average MW = 2200 g/mol).* The titled product was obtained without purification as a white solid (3.20 g, 100%), following Procedure E, using polyethyeneglycol methyl ether tosylate (average MW = 2000 g/mol) (2400 mg, 1.2 mmol) and 3,5-difluoro-4-(hydroxymethyl)phenol (211 mg, 1.32 mmol). ^{1}H NMR (300 MHz, DMSO-d_6): δ (ppm) 3.23 (s, 3H), 3.36−3.76 (m, 278H), 4.06−4.14 (m, 2H), 4.40 (brs, 2H), 5.08 (brs, 1H), 6.56−6.76 (m, 2H).

*2-(Chloromethyl)-1,3-difluoro-5-(2-methoxypolyethyleneglycoxy]benzene (**P5ii**) (Average MW = 2220 g/mol).* The titled product was obtained (2.94 g, 100%), following Procedure F, using [2,6-difluoro-4-(methoxypolyethyleneglycoxy)-phenyl]methanol **P5i** (2.91 g, 1.47 mmol).

2-[2-[2,6-Difluoro-4-(methoxypolyethyleneglycoxy)benzyl]-3-(4-fluorophenyl)isothioureido]-N-(3,4-dimethoxyphenyl)-N-methylacetamide (P5a) (Average MW = 2413 g/mol). The titled product was obtained as a yellow solid (693 mg, 20%), following Procedure A, using 2-(chloromethyl)-1,3-difluoro-5-(2-methoxypolyethyleneglycoxy]benzene **P5ii** (2.94 g, 1.47 mmol) and *N*-(3,4-dimethoxyphenyl)-2-[3-(4-fluorophenyl) isothioureido]-*N*-methylacetamide (**1d**) (553 mg, 1.47 mmol). LC-MS: t_R = 3.54 min. MS [M + H + $3H_3O$]$^{4+}$ m/z = 609.4 (n = 42).

*[2-[2,6-Difluoro-4-(2-methoxypolyethyleneglycoxy)-benzylsulfanyl]-3-(4-fluorophenyl)-3H-imidazol-4-yl]-(3,4-dimethoxyphenyl)methylamine (**P5**) (average MW = 2347 g/mol, n = 34−52).* The titled product was obtained after purification by

https://dx.doi.org/10.1021/acs.jmedchem.0c01774
J. Med. Chem. 2021, 64, 1593−1610

preparative HPLC as a yellowish solid (110 mg, 16%), following Procedure B, using 2-[2-[2,6-difluoro-4-(methoxypolyethyleneglycoxy)benzyl]-3-(4-fluorophenyl)-isothioureido]-*N*-(3,4-dimethoxyphenyl)-*N*-methyl-acetamide **P5a** (693 mg, 287 μmol). LC-MS: t_R = 3.02 min. MS [M + H + $2H_3O$]$^{3+}$ *m*/*z* = 786.0 (*n* = 41). ^{1}H NMR (300 MHz, CD_2Cl_2): δ (ppm) 2.96 (s, 3H), 3.36−3.87 (m, 213H), 4.04−4.11 (m, 4H), 6.15 (dd, *J* = 8.7, 2.8 Hz, 1H), 6.27 (d, *J* = 2.8 Hz, 1H), 6.41−6.50 (m, 2H), 6.72 (d, *J* = 8.7 Hz, 1H), 6.96−7.07 (m, 5H). ^{13}C NMR (75 MHz, CD_2Cl_2): δ (ppm) 25.8, 40.1, 55.8, 56.4, 58.6, 68.3, 69.2, 70.3, 70.4, 70.5, 70.8, 71.9, 98.1−98.7 (m), 100.1, 105.5, 105.6 (t, *J* = 20.5 Hz), 112.9, 115.7 (d, *J* = 23.0 Hz), 124.0, 129.3 (d, *J* = 8.9 Hz), 131.1 (d, *J* = 3.3 Hz), 138.0, 139.8, 142.8, 143.3, 149.8; 159.7 (t, *J* = 14.5 Hz), 161.6 (dd, *J* = 247.1, 11.3 Hz), 162.3 (d, *J* = 248.3 Hz).

*2,6-Difluoro-4-(methoxypolyethyleneglycoxy)phenyl]methanol (**P6i**) (Average MW = 916 g/mol).* The titled product was obtained as a white viscous residue (893 mg, 63%), following Procedure E, using polyethyeneglycol methyl ether tosylate (average MW = 900 g/mol) (1.32 g, 1.46 mmol) and 3,5-difluoro-4-(hydroxymethyl)phenol (260 mg, 1.62 mmol). LC-MS: t_R = 2.23 min. MS [M + H_3O]$^+$ *m*/*z* = 896.6 (*n* = 16).

*2-(Chloromethyl)-1,3-difluoro-5-(2-methoxypolyethyleneglycoxy]benzene (**P6ii**) (Average MW = 935 g/mol).* The titled product was obtained (912 mg, 100%), following Procedure E, using 2,6-difluoro-4-(methoxypolyethyleneglycoxy)-phenyl]methanol **P6i** (893 mg, 1.02 mmol). LC-MS: t_R = 2.75 min. MS [M + H_3O]$^+$ *m*/*z* = 914.5 (*n* = 16).

*2-[2-[2,6-Difluoro-4-(methoxypolyethyleneglycoxy)benzyl]-3-(4-fluoro-3-methoxyphenyl)isothioureido]-N-(3,4-dimethoxyphenyl)-N-methylacetamide (**P6a**) (Average MW = 1209 g/mol).* The titled product was obtained after purification by preparative HPLC as a pale pink solid (333 mg, 26%), following Procedure A, using 2-(chloromethyl)-1,3-difluoro-5-(2-methoxypolyethyleneglycoxy]-benzene **P6ii** (912 mg, 1.02 mmol)) and *N*-(3,4-dimethoxyphenyl)-2-[3-(4-fluoro-3-methoxyphenyl)isothioureido]-*N*-methylacetamide (**2d**) (414 mg, 1.02 mmol). LC-MS: t_R = 2.85 min. MS [M + H + H_3O]$^{2+}$ *m*/*z* = 643.5 (*n* = 16). ^{1}H NMR (300 MHz, CD_2Cl_2): δ (ppm) 3.29 (s, 3H), 3.35 (s, 3H), 3.50−3.72 (m, 80H), 3.80−3.90 (m, 13H), 4.03−4.17 (m, 4H), 6.32 (brs, 1H), 6.46−6.56 (m, 3H), 6.70−7.02 (m, 5H).

*[2-[2,6-Difluoro-4-(2-methoxypolyethyleneglycoxy)-benzylsulfanyl]-3-(4-fluoro-3-methoxyphenyl)-3H-imidazol-4-yl]-(3,4-dimethoxyphenyl)methylamine (**P6**) (Average MW = 1329 g/mol, n = 14−24).* The titled product was obtained after purification by preparative HPLC as a pale orange oil (47 mg, 17%), following Procedure C, using 2-[2-[2,6-difluoro-4-(methoxypolyethyleneglycoxy)benzyl]-3-(4-fluoro-3-methoxyphenyl)-isothioureido]-*N*-(3,4-dimethoxyphenyl)-*N*-methylacetamide **P6a** (333 mg, 263 μmol). LC-MS: t_R = 2.90 min. MS [M + H + H_3O]$^{2+}$ *m*/*z* = 678.6 (*n* = 18). ^{1}H NMR (300 MHz, CD_2Cl_2): δ (ppm) 2.93 (s, 3H), 3.36 (s, 3H), 3.48−3.72 (m, 76H), 3.73−3.78 (m, 6H), 3.79−3.85 (m, 2H), 4.04−4.13 (m, 4H), 6.17 (dd, *J* = 8.7, 2.7 Hz, 1H), 6.31 (d, *J* = 2.6 Hz, 1H), 6.40−6.50 (m, 2H), 6.57 (dd, *J* = 7.6, 2.3 Hz, 1H), 6.63−6.70 (m, 1H), 6.75 (d, *J* = 8.7 Hz, 1H), 6.96−7.09 (m, 2H). ^{13}C NMR (75 MHz, CD_2Cl_2): δ (ppm) 25.8, 39.9, 55.8, 55.9, 56.5, 58.6, 68.3, 69.2, 70.4, 70.5, 70.8, 71.9, 98.1−98.5 (m), 99.9, 105.5, 105.6 (t, *J* = 20.2 Hz), 112.9 (d, *J* = 2.5 Hz), 113.1, 115.7 (d, *J* = 19.6 Hz), 119.8 (d, *J* = 7.3 Hz), 124.7, 131.2 (d, *J* = 3.6 Hz), 138.2, 139.3, 142.7, 143.6, 147.6 (d, *J* = 11.6 Hz), 150.0, 151.9 (d, *J* = 247.9 Hz), 159.7 (t, *J* = 14.1 Hz), 161. 7 (dd, *J* = 252.8, 5.6 Hz).

*2-[[(Z)-C-[(4-Bromo-2,6-difluorophenyl)methylsulfanyl]-N-(4-fluoro-3-methoxyphenyl) carbonimidoyl]amino]-N-(3,4-dimethoxyphenyl)-N-methylacetamide (**7a**).* The titled product was obtained as an oily residue (4.02 g, 98%), following Procedure A, using *N*-(3,4-dimethoxyphenyl)-2-[[(*Z*)-*N*-(4-fluoro-3-methoxyphenyl)-*C*-sulfanylcarbonimidoyl]amino]-*N*-methylacetamide (**2d**) (2.74 g, 6.7 mmol) and 5-bromo-2-(chloromethyl)-1,3-difluorobenzene (1.62 g, 6.7 mmol). LC-MS: t_R = 3.40 min. MS [M + H]$^+$ *m*/*z* = 613.0. ^{1}H NMR (300 MHz, $CDCl_3$): δ (ppm) 3.30 (s, 3H), 3.82 (s, 3H), 3.87 (s,3H), 3.91 (s, 3H), 3.85 (s, 2H), 4.07 (s, 2H), 5.80 (s, 1H), 6.31 (s, 1H), 6.44 (s, 1H), 6.70 (s, 1H), 6.78 (d, *J* = 8.3 Hz, 1H), 6.86 (d, *J* = 8.3 Hz, 1H), 6.93 (d, *J* = 9.0 Hz, 1H), 7.03−7.13 (m, 2H).

*2-[(4-Bromo-2,6-difluorophenyl) methylsulfanyl]-N-(3,4-dimethoxyphenyl)-3-(4-fluoro-3-methoxyphenyl)-N-methylimidazol-4-amine (**7b**).* The titled product was obtained as a yellow oil (3.90 g, 100%), following Procedure C, using 2-[[(*Z*)-*C*-[(4-bromo-2,6-difluorophenyl)methylsulfanyl]-*N*-(4-fluoro-3-methoxyphenyl)-carbonimidoyl]amino]-*N*-(3,4-dimethoxyphenyl)-*N*-methylacetamide (**7a**) (4.02 g, 6.56 mmol). LC-MS: t_R = 3.35 min. MS [M + H]$^+$ *m*/*z* = 595.9. ^{1}H NMR (300 MHz, $CDCl_3$): δ (ppm) 2.90 (s, 3H), 3.55 (s, 3H), 3.80 (s, 3H), 3.82 (s, 3H), 4.12 (s, 2H), 6.13−6.18 (dd, *J* = 8.5, 2.8 Hz, 1H), 6.30 (d, *J* = 2.8 Hz, 1H), 6.51−6.54 (dd, *J* = 7.6, 2.6 Hz, 1H), 6.58−6.63 (m, 1H), 6.74 (d, *J* = 8.5 Hz, 1H), 7.00−7.04 (m, 4H).

*4-[4-[[5-(3,4-dimethoxy-N-methylanilino)-1-(4-fluoro-3-methoxyphenyl)imidazol-2-yl]sulfanylmethyl]-3,5-difluorophenyl]-benzoic Acid (**7c**).* The titled product was obtained as a white powder, after purification by preparative HPLC (528 mg, 52%), following Procedure D, using 2-[(4-bromo-2,6-difluorophenyl)-methylsulfanyl]-*N*-(3,4-dimethoxyphenyl)-3-(4-fluoro-3-methoxy-phenyl)-*N*-methylimidazol-4-amine (**7b**) (950 mg, 1.6 mmol) and 4-boronobenzoic acid (265 mg, 1.6 mmol). LC-MS: t_R = 2.97 min. MS [M + H]$^+$ *m*/*z* = 636. ^{1}H NMR (300 MHz, DMSO-d_6): δ (ppm) 2.92 (s, 3H), 3.48 (s, 3H), 3.59 (s, 3H), 3.65 (s, 3H), 4.13 (s, 2H), 6.06 (dd, *J* = 8.8, 2.8 Hz, 1H), 6.24 (d, *J* = 2.8 Hz, 1H), 6.61−6.67 (m, 1H), 6.75 (d, *J* = 8.8 Hz, 1H), 6.78 (dd, *J* = 7.9, 2.5 Hz, 1H), 7.02 (s, 1H), 7.17 (dd, *J* = 11.4, 8.4 Hz, 1H), 7.52 (d, *J* = 9.2 Hz, 2H), 7.87 (d, *J* = 8.4 Hz, 2H), 8.01 (d, *J* = 8.4 Hz, 2H), 13.08 (s, 1H).

*4-[4-[[5-(3,4-Dimethoxy-N-methylanilino)-1-(4-fluoro-3-methoxyphenyl)imidazol-2-yl]sulfanylmethyl]-3,5-difluorophenyl]-N-[2-[2-methoxypolyethyleneglycoxy]ethyl]benzamide (**P7**) (Average MW = 1081 g/mol, n = 4−13).* In a 5 mL flask were added **7c** (100 mg, 0.16 mmol), TEA (21.23 μL, 0.16 mmol), DCC (32.46 mg, 0.16 mmol), HOBt (21.26 mg, 0.16 mmol), and 2-[2-methoxypolyethyleneglycoxy]ethanamine (average MW = 500 g/mol) (74.19 mg, 0.16 mmol) in 1 mL of DCM. The reaction mixture was stirred overnight at room temperature. The reaction mixture was evaporated and purified by preparative HPLC to give the titled product as a white powder (106 mg, 62%). LC-MS: t_R = 2.88 min. MS [M + H]$^+$ *m*/*z* = 1089 (*n* = 10). ^{1}H NMR (300 MHz, CD_2Cl_2): δ (ppm) 2.94 (s, 3H), 3.35 (s, 3H), 3.53 (s, 3H), 3.56−3.64 (m, 24H), 3.65−3.68 (m, 8H), 3.75 (s, 3H), 3.77 (s, 3H), 4.20 (s, 2H), 6.18 (dd, *J* = 8.7, 2.8 Hz, 1H), 6.32 (d, *J* = 2.8 Hz, 1H), 6.61 (dd, *J* = 7.7, 2.6 Hz, 1H), 6.63−6.69 (m, 1H), 6.73 (d, *J* = 8.7 Hz, 1H), 7.00 (d, *J* = 10.9, 8.5 Hz, 1H), 7.02 (s, 1H), 7.16 (d, *J* = 8.6 Hz, 2H), 7.63 (d, *J* = 8.6 Hz, 2H), 7.92 (d, *J* = 8.6 Hz, 2H). ^{13}C NMR (75 MHz, CD_2Cl_2): δ (ppm) 25.4, 34.3, 40.3, 56.2, 56.3, 56.9, 70.2, 70.9, 72.2, 100.5, 105.8, 110.2 (m), 113.4 (t, *J* = 9.3 Hz), 113.5, 116.1 (d, *J* = 19.5 Hz), 120.1 (d, *J* = 7.0 Hz), 125.1, 127.1, 128.3, 131.5 (d, *J* = 4.2 Hz), 135.2, 138.3, 139.8, 141.2, 142.2, 143.2, 143.9, 148.1 (d, *J* = 12.5 Hz), 150.3, 152.4 (d, *J* = 248.1 Hz), 161.8 (dd, *J* = 248.1, 8.9 Hz), 166.8.

*[4-[2-[2-Methoxypolyethyleneglycoxy]ethylcarbamoyl]phenyl]-boronic Acid (**P8i**) (Average MW = 1009 g/mol, n = 15−21).* In a 25 mL flask were added 4-boronobenzoic acid (30 mg, 0.18 mmol), 2-[2-methoxypolyethyleneglycoxy]ethanamine (average MW = 750 g/mol) (141.01 mg, 0.18 mmol), HOBt (24.5 mg, 0.18 mmol), DCC (37.3 mg, 0.18 mmol), and 25 μL of TEA in 400 μL of dichloromethane. The reaction mixture was stirred at room temperature overnight. The reaction mixture was concentrated under reduced pressure, and the residue was diluted in ethyl acetate and washed with water. The aqueous layer was extracted with dichloromethane, dried over Na_2SO_4, filtered, and concentrated under reduced pressure to give the titled product as a colorless oil (110 mg, 66%). It was used without further purification in the next step of the synthesis. LC-MS: t_R = 2.40 min. MS [M + H_3O]$^+$ *m*/*z* = 990 (*n* = 18). ^{1}H NMR (300 MHz, DMSO-d_6): δ (ppm) 3.23 (s, 3H), 3.32 (s, 4H), 3.40−3.44 (m, 4H), 3.45−3.60 (m, 62H), 7.78 (d, *J* = 8.2 Hz, 2H), 7.84 (d, *J* = 8.2 Hz, 2H), 8.17 (s, 1H).

4-[4-[[5-(3,4-Dimethoxy-N-methylanilino)-1-(4-fluoro-3-methoxyphenyl)imidazol-2-yl]sulfanylmethyl]-3,5-difluorophenyl]-

https://dx.doi.org/10.1021/acs.jmedchem.0c01774
J. Med. Chem. 2021, 64, 1593−1610

*N-[2-[2-methoxypolyethyleneglycoxy]ethyl]benzamide (**P8**) (Average MW = 1394 g/mol, n = 12−24).* The titled product was obtained as an oily residue, after purification by preparative HPLC (40 mg, 43%), following Procedure D, using **7c** (40 mg, 67 μmol) and [4-[2-[2-methoxypolyethyleneglycoxy]ethylcarbamoyl]phenyl]boronic acid **P8i** (62. 4 mg, 67 μmol). LC-MS: t_R = 3.02 min. MS $[M + H]^+$ m/z = 1353 (n = 16). ^{1}H NMR (300 MHz, CD_2Cl_2): δ (ppm) 2.91 (s, 3H), 3.33 (s, 3H), 3.50 (s, 3H), 3.48−3.51 (m, 2H), 3.53−3.70 (m, 72H), 3.72 (s, 3H), 3.74 (s, 3H), 4.17 (s, 2H), 6.13−6.17 (dd, J = 8.7, 2.8 Hz, 1H), 6.29 (d, J = 2.8 Hz, 1H), 6.57−6.60 (dd, J = 7.9, 2.4 Hz, 1H), 6.61−6.60 (m, 1H), 6.71 (d, J = 8.7 Hz, 1H), 6.96 (d, J = 8.4 Hz, 1H), 7.00 (s, 1H), 6.99 (d, J = 8.4 Hz, 1H), 7.13 (d, J = 8.4 Hz, 2H), 7.61 (d, J = 8.4 Hz, 2H), 7.90 (d, J = 8.4 Hz, 1H). ^{13}C NMR (75 MHz, CD_2Cl_2): δ (ppm) 26.2, 40.3, 56.2, 56.3, 56.9, 59.0, 70.1, 70.7, 70.8, 70.9, 72.3, 100.4, 105.8, 109.8−110.5 (m), 113.4 (d, J = 2.6 Hz), 113.5, 113.5 (t, J = 19.7 Hz), 116.1 (d, J = 19.8 Hz), 120.1 (d, J = 7.2 Hz), 125.1, 127.2, 128.3, 131.6 (d, J = 3.5 Hz), 135.2, 138.3, 139.8, 141.2 (t, J = 1.7 Hz), 142.1 (t, J = 9.8 Hz), 143.2, 144.0, 148.0 (d, J = 11.5 Hz), 150.4, 152.4 (d, J = 247.9 Hz), 161.8 (dd, J = 248.9, 8.6 Hz), 166.8.

*4-[4-[[5-(3,4-Dimethoxy-N-methylanilino)-1-(4-fluoro-3-methoxyphenyl)imidazol-2-yl]sulfanylmethyl]-3,5-difluorophenyl]-N-[2-[2-methoxypolyethyleneglycoxy]ethyl]benzamide (**P9**) (Average MW = 1452 g/mol, n = 11−25).* In a 5 mL flask were added 4-[4-[[5-(3,4-dimethoxy-*N*-methylanilino)-1-(4-fluoro-3-methoxyphenyl)imidazol-2-yl]sulfanylmethyl]-3,5-difluorophenyl]-benzoic acid (**7c**) (80 mg, 0,13 mmol), 2-[2-methoxypolyethyleneglycoxy]ethanamine (average MW = 750 g/mol) (98 mg, 0,13 mmol), HOBt (17 mg, 0,13 mmol), DCC (19 mg, 0,13 mmol), and TEA (18 μL, 0,13 mmol). The reaction mixture was stirred at room temperature for 48 h. The reaction mixture was evaporated to dryness. The crude was purified by preparative chromatography to give the desired product as a colorless oil (127 mg, 72%). LC−MS: t_R = 2.73 min. MS $[M + H]^+$ m/z = 1398 (n = 17). ^{1}H NMR (300 MHz, CD_2Cl_2): δ (ppm) 2.90 (s, 3H), 3.31 (s, 3H), 3.48 (s, 3H), 3.58 (m, 68H), 3.70 (s, 3H), 3.73 (s, 3H), 4.15 (s, 2H), 6.13 (d, J = 8.6 Hz, 1H), 6.28 (s, 1H), 6.56−6.63 (m, 2H), 6.68 (d, J = 8.7 Hz, 1H), 6.94 (d, J = 11.0 Hz, 1H), 6.99 (s, 1H), 7.10 (d, J = 8.0 Hz, 2H), 7.32 (s, 1H), 7.58 (d, J = 8.2 Hz, 2H), 7.90 (d, J = 8.1 Hz, 2H). ^{13}C NMR (75 MHz, CD_2Cl_2): δ (ppm) 26.2, 40.2, 56.1, 56.2, 56.8, 58.9, 70.1, 70.5, 70.6, 70.8, 72.2, 100.4, 105.8, 110.1 (d, J = 25.6 Hz), 113.3 (d, J = 2.9 Hz), 113.4, 113.4 (t, J = 20.0 Hz), 116.0 (d, J = 19.8 Hz), 120.1 (d, J = 7.2 Hz), 125.0, 127.0, 128.3, 131.5 (d, J = 3.6 Hz), 135.1, 138.2, 139.7, 141.0, 142.1 (t, J = 10.2 Hz), 143.1, 143.9, 147.9 (d, J = 11.4 Hz), 150.3, 152.3 (d, J = 248.1 Hz), 161.7 (dd, J = 249.0, 8.9 Hz), 166.7.

*[4-[2-[2-Methoxypolyethyleneglycoxy]ethylcarbamoyl]phenyl]-boronic Acid (**P10i**) (Average MW = 2164 g/mol, n = 36−53).* In a 25 mL flask were added 4-boronobenzoic acid (20 mg, 0.12 mmol), 2-[2-methoxypolyethyleneglycoxy]ethanamine (average MW = 2000 g/mol) (243 mg, 0.12 mmol), HOBt (17 mg, 0.12 mmol), DCC (25 mg, 0.12 mmol), and TEA (16.26 μL, 0.12 mmol) in 400 μL of dichloromethane. The reaction mixture was stirred at room temperature overnight. HOBt (17 mg, 0.12 mmol), DCC (25 mg, 0.12 mmol), and TEA (16.26 μL, 0.12 mmol) were added again in the reaction mixture, and it was stirred at room temperature for 24 h at 40 °C. The reaction mixture was filtered and concentrated under reduced pressure. Purification of the crude by preparative HPLC gave the titled product as a white powder (166 mg, 64%). LC-MS: t_R = 2.55 min. MS $[M + 2H_3O]^+$ m/z = 1098.5 (n = 45). ^{1}H NMR (300 MHz, CD_2Cl_2): δ (ppm) 3.36 (s, 3H), 3.47−3.75 (m, 176H), 6.27(s, 2H), 7.04 (s, 1H), 7.79 (d, J = 7.6 Hz, 2H), 7.91 (d, J = 7.6 Hz, 2H).

*4-[4-[[5-(3,4-Dimethoxy-N-methylanilino)-1-(4-fluoro-3-methoxyphenyl)imidazol-2-yl]sulfanylmethyl]-3,5-difluorophenyl]-N-[2-[2-methoxypolyethyleneglycoxy]ethyl]benzamide (**P10**) (Average MW = 2608 g/mol, n = 33−57).* The titled product was obtained as an oily residue after a purification by preparative HPLC (93 mg, 47%), following Procedure D, using **7c** (45 mg, 76 μmol) and [4-[2-[2-methoxypolyethyleneglycoxy]ethylcarbamoyl]phenyl]-boronic acid **P10i** (163.6 mg, 76 μmol). LC-MS: t_R = 2.93 min. MS $[M + H + H_3O]^{2+}$ m/z = 1347 (n = 46). ^{1}H NMR (300 MHz, CD_2Cl_2): δ (ppm) 3.33 (s, 3H), 3.49 (s, 3H), 3.51−3.66 (m, 180H), 3.71 (s, 3H), 3.74 (s, 3H), 4.16 (s, 2H), 6.12−6.16 (dd, J = 8.6, 2.7 Hz, 1H), 6.29 (d, J = 2.7 Hz, 1H), 6.55−6.64 (m, 2H), 6.69 (d, J = 8.6 Hz, 1H), 6.94−7.00 (dd, J = 10.8, 8.4 Hz, 1H), 6.99 (s, 1H), 7.10−7.14 (m, 1H), 7.13 (d, J = 8.4 Hz, 2H), 7.59 (d, J = 8.6 Hz, 2H), 7.89 (d, J = 8.6 Hz, 2H). ^{13}C NMR (75 MHz, CD_2Cl_2): δ (ppm) 25.9, 39.9, 55.8, 55.9, 56.5, 58.6, 69.7, 70.3, 70.4, 70.5, 71.8, 100.1, 105.5, 109.5−110.0 (m), 113.0 (d, J = 3.0 Hz), 113.1 (t, J = 19.6 Hz), 113.1, 115.7 (d, J = 19.2 Hz), 119.8 (d, J = 7.3 Hz), 124.7, 126.8, 127.9, 131.1 (d, J = 3.5 Hz), 134.8, 137.9, 139.4, 140.8 (t, J = 2.3 Hz), 141.8 (t, J = 9.9 Hz), 142.8, 143.5, 147.6 (d, J = 11.7 Hz), 150.0, 152.0 (d, J = 248.1 Hz), 161.4 (dd, J = 249.2, 8.8 Hz), 166.4.

*4-[4-[[5-(3,4-Dimethoxy-N-methylanilino)-1-(4-fluoro-3-methoxyphenyl)imidazol-2-yl]sulfanylmethyl]-3,5-difluorophenyl]-N-[2-[2-methoxypolyethyleneglycoxy]ethyl]benzamide (**P11**) (Average MW = 2574 g/mol, n = 31−57).* In a 5 mL flask were added 4-[4-[[5-(3,4-dimethoxy-*N*-methylanilino)-1-(4-fluoro-3-methoxyphenyl)imidazol-2-yl]sulfanylmethyl]-3,5-difluorophenyl]-benzoic acid (**7c**) (150 mg, 0.24 mmol), 2-[2-methoxypolyethyleneglycoxy]ethanamine (average MW = 2000 g/mol) (486 mg, 0.24 mmol), HOBt (32 mg, 0.24 mmol), DCC (49 mg, 0.24 mmol), and TEA (33 μL, 0.24 mmol). The reaction mixture was stirred overnight at room temperature. The reaction mixture was evaporated to dryness. The crude was purified by preparative chromatography to give the desired product as a yellow powder (263 mg, 42%). LC-MS: t_R = 2.76 min. MS $[M + H + H_3O]^{2+}$ m/z = 1346.7 (n = 46). ^{1}H NMR (300 MHz, CD_2Cl_2): δ (ppm) 2.89 (s, 3H), 3.31 (s, 3H), 3.48 (s, 3H), 3.58 (m, 182H), 3.70 (s, 3H), 3.73 (s, 3H), 4.14 (s, 2H), 6.11−6.15 (dd, J = 8.7, 2.8 Hz, 1H), 6.27 (d, J = 2.8 Hz, 1H), 6.54 (dd, J = 7.6, 2.4 Hz, 1H), 6.58−6.63 (m, 1H), 6.68 (d, J = 8.8 Hz, 1H), 6.93−7.00 (dd, J = 10.9, 8.5 Hz, 1H), 6.98 (s, 1H), 7.10 (d, J = 8.5 Hz, 2H), 7.14 (s, 1H), 7.58 (d, J = 8.6 Hz, 2H), 7.88 (d, J = 8.6 Hz, 2H). ^{13}C NMR (75 MHz, CD_2Cl_2): δ (ppm) 25.9, 39.9, 55.8, 55.9, 56.5, 58.6, 69.7, 70.3, 70.4, 70.5, 71.8, 100.1, 105.5, 109.5−110.0 (m), 113.0 (d, J = 3.0 Hz), 113.1 (t, J = 19.6 Hz), 113.1, 115.7 (d, J = 19.2 Hz), 119.8 (d, J = 7.3 Hz), 124.7, 126.8, 127.9, 131.1 (d, J = 3.5 Hz), 134.8, 137.9, 139.4, 140.8 (t, J = 2.3 Hz), 141.8 (t, J = 9.9 Hz), 142.8, 143.5, 147.6 (d, J = 11.7 Hz), 150.0, 152.0 (d, J = 248.1 Hz), 161.4 (dd, J = 248.2, 8.8 Hz), 166.4.

*4-[4-[[5-(3,4-Dimethoxy-N-methylanilino)-1-(4-fluoro-3-methoxyphenyl)imidazol-2-yl]sulfanylmethyl]-3,5-difluorophenyl]-N-[2-[2-methoxypolyethyleneglycoxy]ethyl]benzamide (**P12**) (Average MW = 5831 g/mol, m = 100−138).* In a 5 mL flask were added **7c** (80 mg, 0.13 mmol), TEA (17 μL, 0.13 mmol), DCC (26 mg, 0.13 mmol), HOBt (17 mg, 0.13 mmol), and 2-[2-methoxy polyethyleneglycoxy]ethanamine (average MW = 5000 g/mol) (614 mg, 0.13 mmol) in 1 mL of DCM. The reaction mixture was stirred overnight at room temperature. The reaction mixture was evaporated and purified by preparative HPLC to give the titled product as a white powder (465 mg, 67%). LC-MS: t_R = 2.65 min. MS $[M + 3H + H_3O]^{4+}$ m/z = 1377.5 (n = 110). ^{1}H NMR (300 MHz, CD_2Cl_2): δ (ppm) 2.93 (s, 3H), 3.35 (s, 3H), 3.50−3.80 (m, 480H), 3.68 (s, 3H), 3.72 (s, 3H), 3.76 (s, 3H), 4.22 (brs, 2H), 6.17 (dd, J = 8.8, 2.8 Hz, 1H), 6.30 (d, J = 2.8 Hz, 1H), 6.55 (brs, 1H), 6.71 (d, J = 8.8 Hz, 1H), 6.93 (brs, 1H), 7.00−7.27 (m, 4H), 7.60 (d, J = 8.3 Hz, 2H), 7.93 (d, J = 8.3 Hz, 2H). ^{13}C NMR (75 MHz, CD_2Cl_2): δ (ppm) 25.5, 34.3, 40.4, 56.5, 56.7, 56.9, 70.1, 70.8, 72.2, 100.6, 105.7, 110.3 (m), 113.4 (t, J = 9.3 Hz), 113.6, 116.3 (d, J = 19.5 Hz), 120.5 (d, J = 7.0 Hz), 125.2, 127.1, 128.3, 131.4 (d, J = 4.2 Hz), 135.2, 138.2, 139.9, 141.3, 142.2, 143.1, 143.9, 148.4 (d, J = 12.5 Hz), 150.3, 152.6 (d, J = 248.1 Hz), 161.7 (dd, J = 248.1, 8.9 Hz), 166.6.

*4-[4-[[5-(3,4-Dimethoxy-N-methylanilino)-1-(4-fluoro-3-methoxyphenyl)imidazol-2-yl]sulfanylmethyl]-3,5-difluorophenyl]-N-[2-[2-[2-[2-(2-methoxyethoxy)ethoxy]ethoxy]ethoxy]ethyl]-benzamide (**13**, n = 5).* In a 10 mL flask were **7c** (58 mg, 0,091 mmol), Et_3N (12.3 μL, 0,069 mmol), DIC (14.3 μL, 0,091 mmol), HOBt (12.3 mg, 0,091 mmol), and mPEG5-NH_2 (22.9 mg, 0,091 mmol) in 1 mL of DCM. The reaction mixture was stirred overnight at room temperature. The crude mixture was purified by preparative HPLC to give the titled product (18 mg, 22.5%) as a yellow oil.

https://dx.doi.org/10.1021/acs.jmedchem.0c01774
J. Med. Chem. 2021, 64, 1593−1610

LC−MS: t_R = 3.34 min. MS: $[M + H]^+$ m/z = 869.5. ^{1}H NMR (300 MHz, CD_2Cl_2): δ (ppm) 2.92 (s, 3H), 3.29 (s, 3H), 3.44−3.48 (m, 2H), 3.50 (s, 3H), 3.52−3.57 (m, 6H), 3.58−3.62 (m, 4H), 3.61−3.66 (m, 8H), 3.72 (s, 3H), 3.75 (s, 3H), 4.17 (s, 2H), 6.15 (dd, J = 8.6, 2.8 Hz, 1H), 6.29 (d, J = 2.7 Hz, 1H), 6.59 (dd, J = 7.7, 2.6 Hz, 1H), 6.59−6.66 (m, 1H), 6.71 (d, J = 8.7 Hz, 1H), 6.98 (dd, J = 11.0, 8.5 Hz, 1H), 7.00 (s, 1H), 7.13 (d, J = 8.5 Hz, 2H), 7.61 (d, J = 8.6 Hz, 2H), 7.90 (d, J = 8.6 Hz, 2H). ^{13}C NMR (75 MHz, CD_2Cl_2): δ (ppm) 26.2, 40.3, 40.3, 56.3, 56.4, 56.9, 59.0, 70.2, 70.7, 70.7, 70.9, 72.2, 100.4, 105.8, 110.2, 113.2−113.6, 113.5, 116.1 (d, J = 19.5 Hz), 120.2 (d, J = 7.2 Hz), 125.1, 127.2, 128.3, 131.6 (d, J = 3.6 Hz), 135.2, 138.3, 139.8, 141.2, 142.2 (t, J = 10.1 Hz), 143.2, 144.0, 148.0 (d, J = 11.6 Hz), 150.4, 152.4 (d, J = 248 Hz), 161.8 (dd, J = 249, 8.5 Hz), 166.8.

*4-[4-[[5-(3,4-Dimethoxy-N-methylanilino)-1-(4-fluoro-3-methoxyphenyl)imidazol-2-yl]sulfanylmethyl]-3,5-difluorophenyl]-N-[2-[2-[2-[2-[2-[2-(2-methoxyethoxy)ethoxy]ethoxy]ethoxy]-ethoxy]ethoxy]ethyl]benzamide (**14**, n = 7).* In a 10 mL flask were **7c** (44 mg, 0,069 mmol), Et_3N (9.3 μL, 0,069 mmol), DIC (10.8 μL, 0,069 mmol), HOBt (9.3 mg, 0,069 mmol), and mPEG7-NH_2 (23.5 mg, 0,069 mmol) in 1 mL of DCM. The reaction mixture was stirred overnight at room temperature. The crude mixture was purified by preparative HPLC to give the titled product (37 mg, 54%) as a yellow oil.

LC-MS: t_R = 3.30 min. MS: $[M + H]^+$ m/z = 957.5 ^{1}H NMR (300 MHz, CD_2Cl_2): δ (ppm) 2.92 (s, 3H), 3.32 (s, 3H), 3.47−3.51 (m, 2H), 3.50 (s, 3H), 3.55−3.58 (m, 14H), 3.59−3.62 (m, 4H), 3.62−3.68 (m, 8H), 3.72 (s, 3H), 3.75 (s, 3H), 4.17 (s, 2H), 6.14 (dd, J = 8.6, 2.7 Hz, 1H), 6.28 (d, J = 2.7 Hz, 1H), 6.58 (dd, J = 7.5, 2.5 Hz, 1H), 6.59−6.64 (m, 1H), 6.70 (d, J = 8.6 Hz, 1H), 6.97 (dd, J = 10.9, 8.4 Hz, 1H), 6.99 (s, 1H), 7.12 (d, J = 8.6 Hz, 2H), 7.59 (d, J = 8.6 Hz, 2H), 7.90 (d, J = 8.6 Hz, 2H). ^{13}C NMR (75 MHz, CD_2Cl_2): δ (ppm) 26.2, 40.3, 40.3, 56.2, 56.3, 56.9, 59.0, 70.2, 70.6, 70.7, 70.8, 72.2, 100.4, 105.8, 110.0−110.4 (m), 113.2−113.5 (m), 113.4, 116.1 (d, J = 19.6 Hz), 120.1 (d, J = 7.4 Hz), 125.1, 127.2, 128.3, 131.6 (d, J = 3.6 Hz), 135.2, 138.3, 139.8, 141.2 (m), 142.1 (t, J = 10.2 Hz), 143.1, 143.9, 148.0 (d, J = 11.6 Hz), 150.3, 152.3 (d, J = 248 Hz), 161.8 (dd, J = 249, 8.8 Hz), 166.8.

*4-[4-[[5-(3,4-Dimethoxy-N-methylanilino)-1-(4-fluoro-3-methoxyphenyl)imidazol-2-yl]sulfanylmethyl]-3,5-difluorophenyl]-N-[2-[2-[2-[2-[2-[2-[2-(2-methoxyethoxy)ethoxy]ethoxy]ethoxy]-ethoxy]ethoxy]ethyl]benzamide (**15**, n = 9).* In a 10 mL flask were added **7c** (100 mg, 0,16 mmol), NEt_3 (21,23 μL, 0,16 mmol), DCC (32,46 mg, 0,16 mmol), HOBt (21,26 mg, 0,16 mmol), and mPEG9-NH_2 (74,19 mg, 0,16 mmol) in 1 mL of DCM. The reaction mixture was stirred 18 h at room temperature and concentrated.The crude mixture was purified by preparative HPLC to give the titled product (70 mg, 41.5%) as a yellow oil. LC-MS: t_R = 2.85 min. MS: $[M + H]^+$ m/z = 1045.7. ^{1}H NMR (300 MHz, CD_2Cl_2): δ (ppm) 2.90 (s, 3H), 3.31 (s, 3H), 3.46−3.50 (m, 2H), 3.49 (s, 3H), 3.54−3.58 (m, 22H), 3.58−3.60 (m, 4H), 3.61−3.66 (m, 8H), 3.71 (s, 3H), 3.73 (s, 3H), 4.16 (s, 2H), 6.14 (dd, J = 8.6, 2.7 Hz, 1H), 6.28 (d, J = 2.7 Hz, 1H), 6.58 (dd, J = 7.5, 2.5 Hz, 1H), 6.59−6.64 (m, 1H), 6.70 (d, J = 8.6 Hz, 1H), 6.97 (dd, J = 10.9, 8.4 Hz, 1H), 6.99 (s, 1H), 7.12 (d, J = 8.6 Hz, 2H), 7.59 (d, J = 8.6 Hz, 2H), 7.90 (d, J = 8.6 Hz, 2H).^{13}C NMR (75 MHz, CD_2Cl_2): δ (ppm) 26.3, 40.3, 56.3, 56.3, 56.9, 59.0, 70.2, 70.7, 70.8, 70.9, 72.3, 100.5, 105.9, 110.2 (m, CH), 113.4 (dd, J = 9.3, 9.2 Hz), 113.5, 116.1 (d, J = 19.4 Hz), 120.1 (d, J = 7.0 Hz, CH), 125.1, 127.2, 128.3, 131.6 (d, J = 3.6 Hz), 135.2, 138.3, 139.8, 141.2 (m), 142.2 (t, J = 9.9 Hz), 143.2, 143.9, 148.0 (d, J = 11.3 Hz), 150.4, 152.3 (d, J = 248 Hz), 161.7 (dd, J = 248, 8.5 Hz), 166.8.

*4-[4-[[5-(3,4-Dimethoxy-N-methylanilino)-1-(4-fluoro-3-methoxyphenyl)imidazol-2-yl]sulfanylmethyl]-3,5-difluorophenyl]-N-[2-[2-[2-[2-[2-[2-[2-[2-[2-(2-methoxyethoxy)ethoxy]ethoxy]-ethoxy]ethoxy]ethoxy]ethoxy]ethoxy]ethoxy]ethyl]-benzamide) (**16**, n = 11).* In a 10 mL flask were added **7c** (116 mg, 0,18 mmol), Et_3N (24.6 μL, 0,18 mmol), DIC (28.6 μL, 0,18 mmol), HOBt (24.7 mg, 0,18 mmol), and mPEG11-NH_2 (94.1 mg, 0,18 mmol) in 1 mL of DCM. The reaction mixture was stirred 18 h at room temperature. The crude mixture was purified by preparative HPLC to give the titled product (79 mg, 38%) as a yellow oil. LC-MS: t_R = 3.25 min. MS: $[M + H]^+$ m/z = 1133.7. ^{1}H NMR (300 MHz, CD_2Cl_2): δ (ppm) 2.91 (s, 3H), 3.32 (s, 3H), 3.47−3.52 (m, 2H), 3.50 (s, 3H), 3.55−3.61 (m, 34H), 3.61−3.68 (m, 8H), 3.71 (s, 3H), 3.74 (s, 3H), 4.17 (s, 2H), 6.15 (dd, J = 8.7, 2.8 Hz, 1H), 6.30 (d, J = 2.8 Hz, 1H), 6.59 (dd, J = 7.7, 2.6 Hz, 1H), 6.61−6.66 (m, 1H), 6.71 (d, J = 8.7 Hz, 1H), 6.98 (dd, J = 11.0, 8.4 Hz, 1H), 7.00 (s, 1H), 7.13 (d, J = 8.7 Hz, 2H), 7.61 (d, J = 8.4 Hz, 2H), 7.91 (d, J = 8.4 Hz, 2H). ^{13}C NMR (75 MHz, CD_2Cl_2): δ (ppm) 26.2, 40.2, 40.3, 56.2, 56.3, 56.8, 58.9, 70.1, 70.7, 70.8, 70.9, 72.2, 100.4, 105.8, 110.0−110.3 (m), 113.0−113.5 (m), 116.1 (d, J = 19.7 Hz), 120.1 (d, J = 7.3 Hz), 125.1, 127.2, 128.3, 131.5 (d, J = 3.7 Hz), 135.1, 138.2, 139.8, 141.1 (m), 142.1 (t, J = 9.8 Hz), 143.1, 143.9, 148.0 (d, J = 12.8 Hz), 150.3, 152.3 (d, J = 248 Hz), 161.8 (dd, J = 249, 8.7 Hz), 166.8.

*4-[4-[[5-(3,4-Dimethoxy-N-methylanilino)-1-(4-fluoro-3-methoxyphenyl)imidazol-2-yl]sulfanylmethyl]-3,5-difluorophenyl]-N-[2-[2-[2-[2-[2-[2-[2-[2-[2-[2-[2-[2-[2-[2-(2-methoxyethoxy)-ethoxy]ethoxy]ethoxy]ethoxy]ethoxy]ethoxy]ethoxy]ethoxy]-ethoxy]ethoxy]ethoxy]ethoxy]ethoxy]ethoxy]ethyl]benzamide) (**17**, n = 16).* In a 10 mL flask were added **7c** (85.5 mg, 0,135 mmol), Et_3N (33.0 μL, 0,245 mmol), DIC (20.8 μL, 0,135 mmol), HOBt (18.2 mg, 0,135 mmol), and mPEG16-NH_2 (90.0 mg, 0,122 mmol) in 3 mL of DCM. The reaction mixture was stirred 18 h at room temperature. The crude mixture was purified by preparative HPLC to give the titled product (29.3 mg, 17.5%) as a yellow oil. LC-MS: t_R = 2.83 min. MS: $[M + H]^+$ m/z = 1353.9. ^{1}H NMR (300 MHz, CD_2Cl_2): δ (ppm) 2.94 (s, 3H), 3.36 (s, 3H), 3.50−3.55 (m, 5H), 3.57−3.54 (m, 54H), 3.65−3.70 (m, 8H), 3.75 (s, 3H), 3.77 (s, 3H), 4.20 (s, 2H), 6.18 (dd, J = 8.7, 2.8 Hz, 1H), 6.32 (d, J = 2.8 Hz, 1H), 6.58−6.69 (m, 2H), 6.74 (d, J = 8.7 Hz, 1H), 6.69−7.05 (m, 2H), 7.09−7.20 (m, 3H), 7.63 (d, J = 8.5 Hz, 2H), 7.93 (d, J = 8.5 Hz, 2H). ^{13}C NMR (75 MHz,CD_2Cl_2): δ (ppm) 26.6, 40.7, 40.7, 56.6, 56.7, 57.3, 59.3, 70.6, 71.0, 71.1, 71.2, 72.6, 100.8, 106.2, 110.4−110.7 (m), 113.7−113.8 (m), 113.9, 116.5 (d, J = 19.6 Hz), 120.5 (d, J = 7.3 Hz), 125.5, 127.5, 128.7, 131.9 (d, J = 3.6 Hz), 135.6, 138.7, 140.2, 141.2 (m), 142.5 (t, J = 10.2 Hz), 143.5, 144.3, 148.4 (d, J = 11.6 Hz), 150.8, 152.7 (d, J = 248.2 Hz), 162.1 (dd, J = 249, 8.9 Hz), 167.2.

*(4-[4-[[5-(3,4-Dimethoxy-N-methylanilino)-1-(4-fluoro-3-methoxyphenyl)imidazol-2-yl]sulfanylmethyl]-3,5-difluorophenyl]-N-[2-[2-[2-[2-[2-[2-[2-[2-[2-[2-[2-[2-[2-[2-[2-[2-[2-[2-[2-[2-(2-methoxyethoxy)ethoxy]ethoxy]ethoxy]-ethoxy]ethoxy]ethoxy]ethoxy]ethoxy]ethoxy]ethoxy]ethoxy]ethoxy]-ethoxy]ethoxy]ethoxy]ethoxy]ethoxy]ethoxy]ethoxy]ethyl]-benzamide) (**18**, n = 24).* In a 10 mL flask were added 4-[4-[[5-(3,4-dimethoxy-*N*-methylanilino)-1-(4-fluoro-3-methoxyphenyl)imidazol-2-yl]sulfanylmethyl]-3,5-difluorophenyl]benzoic acid **7c** (57.8 mg, 0,091 mmol), Et_3N (22.3 μL, 0,165 mmol), DIC (14.2 μL, 0,091 mmol), HOBt (12.3 mg, 0,091 mmol), and mPEG24-NH_2 (90.0 mg, 0,827 mmol) in 1 mL of DCM. The reaction mixture was stirred 18 h at room temperature. The crude mixture was purified by preparative HPLC to give the titled product (73.2 mg, 51%) as yellowish powder. LC-MS: t_R = 2.78 min, MS: $[M + H]^+$ m/z = 1706.1.

^{1}H NMR (300 MHz, CD_2Cl_2): δ (ppm) 2.94 (s, 3H), 3.36 (s, 3H), 3.51−3.54 (m, 5H), 3.58−3.65 (m, 86H), 3.66−3.69 (m, 8H), 3.74 (s, 3H), 3.77(s, 3H), 4.20 (s, 2H), 6.18 (dd, J = 8.7, 2.8 Hz, 1H), 6.32 (d, J = 2.8 Hz, 1H), 6.58−6.68 (m, 2H), 6.74 (d, J = 8.7 Hz, 1H), 6.96−7.05 (m, 2H), 7.16 (d, J = 8.6 Hz, 2H), 7.63 (d, J = 8.5 Hz, 2H), 7.93 (d, J = 8.5 Hz, 2H).

^{13}C NMR (75 MHz, CD_2Cl_2): δ (ppm) 26.6, 40.6, 40.7, 56.6, 56.7, 57.3, 59.4, 70.6, 71.0, 71.1, 71.3, 72.6, 100.8, 106.2, 110.4−110.8 (m), 113.7−113.9 (m), 113.8, 116.5 (d, J = 19.6 Hz), 120.5 (d, J = 7.2 Hz), 125.5, 127.5, 128.7, 132.0 (d, J = 3.6 Hz), 135.6, 138.7, 140.2, 141.2 (m), 142.6 (t, J = 9.8 Hz), 143.5, 144.3, 148.4 (d, J = 11.6 Hz), 150.8, 152.7 (d, J = 248.2 Hz), 162.2 (dd, J = 248.8, 9.0 Hz), 167.3.

(4-[4-[[5-(3,4-Dimethoxy-N-methylanilino)-1-(4-fluoro-3-methoxyphenyl)imidazol-2-yl]sulfanylmethyl]-3,5-difluorophenyl]-N-[2-[2-[2-[2-[2-[2-[2-[2-[2-[2-[2-[2-[2-[2-[2-[2-[2-[2-[2-[2-[2-(2-ethoxyethoxy)ethoxy]ethoxy]ethoxy]-ethoxy]ethoxy]ethoxy]ethoxy]ethoxy]ethoxy]ethoxy]ethoxy]ethoxy]-ethoxy]ethoxy]ethoxy]ethoxy]ethoxy]ethoxy]ethoxy]-

https://dx.doi.org/10.1021/acs.jmedchem.0c01774
J. Med. Chem. 2021, 64, 1593−1610

*ethoxy]ethoxy]ethoxy]ethoxy]ethoxy]ethoxy]ethoxy]ethoxy]ethoxy]ethyl]benzamide) (**19**, n = 36).* In a 10 mL flask were added **7c** (38.9 mg, 0,0612 mmol), Et_3N (15.0 μL, 0,111 mmol), DIC (9.49 μL, 0,0612 mmol), HOBt (8.27 mg, 0,0612 mmol), and mPEG36-NH2 (90.0 mg, 0,0557 mmol) in 1 mL of DCM. The reaction mixture was stirred 18 h at room temperature. The crude mixture was purified by preparative HPLC to give the titled product as a white powder (73.5 mg, 58%). LC-MS: t_R = 2.75 min, MS: $[M + 2H]^{2+}$ m/z = 1226.8. ^1H NMR (300 MHz, CD_2Cl_2): δ (ppm) 2.94 (s, 3H), 3.36 (s, 3H), 3.50−3.54 (m, 5H), 3.58−3.64 (m, 134H), 3.65−3.69 (m, 8H), 3.74 (s, 3H), 3.77(s, 3H), 4.20 (s, 2H), 6.17 (dd, *J* = 8.7, 2.8 Hz, 1H), 6.31 (d, *J* = 2.8 Hz, 1H), 6.58−6.68 (m, 2H), 6.73 (d, *J* = 8.6 Hz, 1H), 6.96−7.05 (m, 2H), 7.16 (d, *J* = 8.6 Hz, 2H), 7.63 (d, *J* = 8.5 Hz, 2H), 7.92 (d, *J* = 8.5 Hz, 2H). ^{13}C NMR (75 MHz, CD_2Cl_2): δ (ppm) 26.6, 40.6, 40.7, 56.6, 56.7, 57.3, 59.4, 70.6, 71.0, 71.1, 71.3, 72.6, 100.8, 106.2, 110.4−110.8 (m), 113.7−113.9 (m), 113.8, 116.5 (d, *J* = 19.6 Hz), 120.5 (d, *J* = 7.2 Hz), 125.5, 127.5, 128.7, 132.0 (d, *J* = 3.6 Hz), 135.6, 138.7, 140.2, 141.6 (m), 142.6 (t, *J* = 9.8 Hz), 143.5, 144.3, 148.4 (d, *J* = 11.4 Hz), 150.7, 152.7 (d, *J* = 248.3 Hz), 162.2 (dd, *J* = 248.8, 9.1 Hz), 167.2.

■ ASSOCIATED CONTENT

Supporting Information

The Supporting Information is available free of charge at https://pubs.acs.org/doi/10.1021/acs.jmedchem.0c01774.

Molecular formula strings (CSV)

■ AUTHOR INFORMATION

Corresponding Authors

Benoit Deprez − *Univ. Lille, Inserm, Institut Pasteur de Lille, U1177 - Drugs and Molecules for Living Systems, EGID, F-59000 Lille, France*; Phone: +33 (0)320 964 924; Email: benoit.deprez@univ-lille.fr

Julie Charton − *Univ. Lille, Inserm, Institut Pasteur de Lille, U1177 - Drugs and Molecules for Living Systems, EGID, F-59000 Lille, France*; orcid.org/0000-0001-6895-276X; Phone: +33 (0)320 964 928; Email: julie.charton@univ-lille.fr

Authors

Vanessa Hoguet − *Univ. Lille, Inserm, Institut Pasteur de Lille, U1177 - Drugs and Molecules for Living Systems, F-59000 Lille, France*

Manuel Lasalle − *Univ. Lille, Inserm, Institut Pasteur de Lille, U1177 - Drugs and Molecules for Living Systems, F-59000 Lille, France*

Mathieu Maingot − *Univ. Lille, Inserm, Institut Pasteur de Lille, U1177 - Drugs and Molecules for Living Systems, F-59000 Lille, France*

Geoffroy Dequirez − *Univ. Lille, Inserm, Institut Pasteur de Lille, U1177 - Drugs and Molecules for Living Systems, F-59000 Lille, France*

Rajaa Boulahjar − *Univ. Lille, Inserm, Institut Pasteur de Lille, U1177 - Drugs and Molecules for Living Systems, F-59000 Lille, France*

Florence Leroux − *Univ. Lille, Inserm, Institut Pasteur de Lille, U1177 - Drugs and Molecules for Living Systems, EGID, F-59000 Lille, France*

Catherine Piveteau − *Univ. Lille, Inserm, Institut Pasteur de Lille, U1177 - Drugs and Molecules for Living Systems, F-59000 Lille, France*

Adrien Herledan − *Univ. Lille, Inserm, Institut Pasteur de Lille, U1177 - Drugs and Molecules for Living Systems, F-59000 Lille, France*

Alexandre Biela − *Univ. Lille, Inserm, Institut Pasteur de Lille, U1177 - Drugs and Molecules for Living Systems, F-59000 Lille, France*

Julie Dumont − *Univ. Lille, Inserm, Institut Pasteur de Lille, U1177 - Drugs and Molecules for Living Systems, F-59000 Lille, France*

Oscar Chávez-Talavera − *Univ. Lille, Inserm, CHU Lille, Institut Pasteur de Lille, U1011 - EGID, F-59000 Lille, France*

Loïc Belloy − *Univ. Lille, Inserm, CHU Lille, Institut Pasteur de Lille, U1011 - EGID, F-59000 Lille, France*

Isabelle Duplan − *Univ. Lille, Inserm, CHU Lille, Institut Pasteur de Lille, U1011 - EGID, F-59000 Lille, France*

Nathalie Hennuyer − *Univ. Lille, Inserm, CHU Lille, Institut Pasteur de Lille, U1011 - EGID, F-59000 Lille, France*

Laura Butruille − *Univ. Lille, Inserm, CHU Lille, Institut Pasteur de Lille, U1011 - EGID, F-59000 Lille, France*

Sophie Lestavel − *Univ. Lille, Inserm, CHU Lille, Institut Pasteur de Lille, U1011 - EGID, F-59000 Lille, France*

Emmanuel Sevin − *Univ. Artois, UR 2465, Blood-brain barrier laboratory (LBHE), F-62300 Lens, France*

Maxime Culot − *Univ. Artois, UR 2465, Blood-brain barrier laboratory (LBHE), F-62300 Lens, France*; orcid.org/0000-0001-7452-0867

Fabien Gosselet − *Univ. Artois, UR 2465, Blood-brain barrier laboratory (LBHE), F-62300 Lens, France*

Bart Staels − *Univ. Lille, Inserm, CHU Lille, Institut Pasteur de Lille, U1011 - EGID, F-59000 Lille, France*

Anne Tailleux − *Univ. Lille, Inserm, CHU Lille, Institut Pasteur de Lille, U1011 - EGID, F-59000 Lille, France*

Complete contact information is available at: https://pubs.acs.org/10.1021/acs.jmedchem.0c01774

Author Contributions

◊J.C. and A.T. contributed equally to this work.

Author Contributions

#M.L. and V.H. contributed equally to this work.

Notes

The authors declare no competing financial interest.

■ ACKNOWLEDGMENTS

We are grateful to the institutions that supported our laboratory: INSERM, Université de Lille, Institut Pasteur de Lille. This project was supported by Conseil Régional Nord-Pas de Calais, ERDF (convention no. 11003609), Etat DRRT, European Genomic Institute for Diabetes (EGID, ANR-10-LABX-46), the European Research Council (ERC Grant Immunobile, contract 694717), European Commission, INSERM, Université Lille 2 (Appel à projets "orientations stratégiques": convention no. A007), and SATT Nord (M0075/SATTNORD), ANR (BABrain, convention n°ANR-17-CE14-0007-03), CPER CTRL17 FEDER TIIMaging. M.L. and V.H. are recipients of a doctoral fellowship of the French Ministère de la Recherche. NMR acquisitions were done at the Laboratoire d'Application de Résonance Magnétique Nucléaire (LARMN), Lille, France. B.S. is honorary member of the Institut Universitaire de France.

■ ABBREVIATIONS USED

BLECs, brain-like endothelial cells; CH_3CN, acetonitrile; DCC, *N,N′*-dicyclohexylcarbodiimide; DCM, dichloromethane; DIC, *N,N′*-diisopropylcarbodiimide; DIEA, diisopropy-

https://dx.doi.org/10.1021/acs.jmedchem.0c01774
J. Med. Chem. 2021, 64, 1593−1610

lethylamine; DME, dimethoxyethane; DMF, *N*,*N*-dimethylformamide; DMSO, dimethyl sulfoxide; EtOAc, ethyl acetate; EtOH, ethanol; equiv., equivalent; GI, gastrointestinal; GLP-1, glucagon-like peptide-1; GP-BAR1, G protein-coupled bile acid receptor 1; PEG, polyethylene glycol; TEA, triethylamine; TCDI, 1,1-thiocarbonyldiimidazole; TGR5, Takeda G protein-coupled receptor 5; THF, tetrahydrofuran; T3P, 1-propylphosphonic acid cyclic anhydride

REFERENCES

(1) Harris, J. M.; Chess, R. B. Effect of pegylation on pharmaceuticals. *Nat. Rev. Drug Discovery* **2003**, *2*, 214−221.

(2) Veronese, F. M.; Pasut, G. PEGylation, successful approach to drug delivery. *Drug Discovery Today* **2005**, *10*, 1451−1458.

(3) Kang, J. S.; DeLuca, P. P.; Lee, K. C. Emerging PEGylated drugs. *Expert Opin. Emerging Drugs* **2009**, *14*, 363−380.

(4) Knop, K.; Hoogenboom, R.; Fischer, D.; Schubert, U. S. Poly(ethylene glycol) in drug delivery: pros and cons as well as potential alternatives. *Angew. Chem., Int. Ed.* **2010**, *49*, 6288−6308.

(5) Bailon, P.; Won, C.-Y. PEG-modified biopharmaceuticals. *Expert Opin. Drug Delivery* **2009**, *6*, 1−16.

(6) Swierczewska, M.; Lee, K. C.; Lee, S. What is the future of PEGylated therapies? *Expert Opin. Emerging Drugs* **2015**, *20*, 531−536.

(7) Turecek, P. L.; Bossard, M. J.; Schoetens, F.; Ivens, I. A. PEGylation of biopharmaceuticals: A review of chemistry and nonclinical safety information of approved drugs. *J. Pharm. Sci.* **2016**, *105*, 460−475.

(8) Li, W.; Zhan, P.; De Clercq, E.; Lou, H.; Liu, X. Current drug research on PEGylation with small molecular agents. *Prog. Polym. Sci.* **2013**, *38*, 421−444.

(9) Park, E. J.; Choi, J.; Lee, K. C.; Na, D. H. Emerging PEGylated non-biologic drugs. *Expert Opin. Emerging Drugs* **2019**, *24*, 107−119.

(10) Asano, S.; Gavrilyuk, J.; Burton, D. R.; Barbas, C. F., III Preparation and activities of macromolecule conjugates of the CCR5 antagonist Maraviroc. *ACS Med. Chem. Lett.* **2014**, *5*, 133−137.

(11) Knauf, M. J.; Bell, D. P.; Hirtzer, P.; Luo, Z. P.; Young, J. D.; Katre, N. V. Relationship of effective molecular size to systemic clearance in rats of recombinant interleukin-2 chemically modified with water-soluble polymers. *J. Biol. Chem.* **1988**, *263*, 15064−15070.

(12) Caliceti, P.; Veronese, F. M. Pharmacokinetic and biodistribution properties of poly(ethylene glycol)-protein conjugates. *Adv. Drug Delivery Rev.* **2003**, *55*, 1261−1277.

(13) Fu, M.; Zhuang, X.; Zhang, T.; Guan, Y.; Meng, Q.; Zhang, Y. PEGylated leuprolide with improved pharmacokinetic properties. *Bioorg.Med. Chem* **2020**, *28*, 115306.

(14) Fishburn, C. S. The pharmacology of PEGylation: balancing PD with PK to generate novel therapeutics. *J. Pharm. Sci.* **2008**, *97*, 4167−4183.

(15) Maruyama, T.; Miyamoto, Y.; Nakamura, T.; Tamai, Y.; Okada, H.; Sugiyama, E.; Nakamura, T.; Itadani, H.; Tanaka, K. Identification of membrane-type receptor for bile acids (M-BAR). *Biochem. Biophys. Res. Commun.* **2002**, *298*, 714−719.

(16) Katsuma, S.; Hirasawa, A.; Tsujimoto, G. Bile acids promote glucagon-like peptide-1 secretion through TGR5 in a murine enteroendocrine cell line STC-1. *Biochem. Biophys. Res. Commun.* **2005**, *329*, 386−390.

(17) Watanabe, M.; Houten, S. M.; Mataki, C.; Christoffolete, M. A.; Kim, B. W.; Sato, H.; Messaddeq, N.; Harney, J. W.; Ezaki, O.; Kodama, T.; Schoonjans, K.; Bianco, A. C.; Auwerx, J. Bile acids induce energy expenditure by promoting intracellular thyroid hormone activation. *Nature* **2006**, *439*, 484−489.

(18) Li, T.; Holmstrom, S. R.; Kir, S.; Umetani, M.; Schmidt, D. R.; Kliewer, S. A.; Mangelsdorf, D. J. The G protein-coupled bile acid receptor, TGR5, stimulates gallbladder filling. *Mol. Endocrinol.* **2011**, *25*, 1066−1071.

(19) Duan, H.; Ning, M.; Chen, X.; Zou, Q.; Zhang, L.; Feng, Y.; Zhang, L.; Leng, Y.; Shen, J. Design, synthesis, and antidiabetic activity of 4-Phenoxynicotinamide and 4-Phenoxypyrimidine-5-carboxamide derivatives as potent and orally efficacious TGR5 agonists. *J. Med. Chem.* **2012**, *55*, 10475−10489.

(20) Fryer, R. M.; Ng, K. J.; Nodop Mazurek, S. G.; Patnaude, L.; Skow, D. J.; Muthukumarana, A.; Gilpin, K. E.; Dinallo, R. M.; Kuzmich, D.; Lord, J.; Sanyal, S.; Yu, H.; Harcken, C.; Cerny, M. A.; Hickey, E. R.; Modis, L. K. G Protein-Coupled Bile Acid Receptor 1 stimulation mediates arterial vasodilation through a KCa1.1 (BKCa)-dependent mechanism. *J. Pharmacol. Exp. Ther.* **2014**, *348*, 421−431.

(21) Lasalle, M.; Hoguet, V.; Hennuyer, N.; Leroux, F.; Piveteau, C.; Belloy, L.; Lestavel, S.; Vallez, E.; Dorchies, E.; Duplan, I.; Sevin, E.; Culot, M.; Gosselet, F.; Boulahjar, R.; Herledan, A.; Staels, B.; Deprez, B.; Tailleux, A.; Charton, J. Topical intestinal aminoimidazole agonists of G-Protein-Coupled Bile Acid Receptor 1 promote Glucagon Like Peptide-1 secretion and improve glucose tolerance. *J. Med. Chem.* **2017**, *60*, 4185−4211.

(22) Kramer, W.; Glombik, H. Bile Acid Reabsorption Inhibitors (BARI): novel hypolipidemic drugs. *Curr. Med. Chem.* **2006**, *13*, 997−1016.

(23) Charmot, D. Non-systemic drugs: a critical review. *Curr. Pharm. Des.* **2012**, *18*, 1434−1445.

(24) Lasalle, M.; Picon, S.; Boulahjar, R.; Hoguet, V.; Van Obbergen, J.; Roussel, P.; Deprez, B.; Charton, J. Access to newly functionalized imidazole derivatives: efficient synthesis of novel 5-amino-2-thioimidazoles using propylphosphonic anhydride (®T3P). *Tetrahedron Lett.* **2015**, *56*, 1011−1014.

(25) Sevin, E.; Dehouck, L.; Versele, R.; Culot, M.; Gosselet, F. A miniaturized pump out method for characterizing molecule interaction with ABC transporters. *Int. J. Mol. Sci.* **2019**, *20*, 5529.

(26) Brighton, C. A.; Rievaj, J.; Kuhre, R. E.; Glass, L. L.; Schoonjans, K.; Holst, J. J.; Gribble, F. M.; Reimann, F. Bile acids trigger GLP-1 release predominantly by accessing basolaterally located G protein-coupled bile acid receptors. *Endocrinology* **2015**, *156*, 3961−3970.

(27) Pedroso, D. C. S.; Tellechea, A.; Moura, L.; Fidalgo-Carvalho, I.; Duarte, J.; Carvalho, E.; Ferreira, L. Improved survival, vascular differentiation and wound healing potential of stem cells co-cultured with endothelial cells. *PLoS One* **2011**, *6*, No. e16114.

(28) Cecchelli, R.; Aday, S.; Sevin, E.; Almeida, C.; Culot, M.; Dehouck, L.; Coisne, C.; Engelhardt, B.; Dehouck, M.-P.; Ferreira, L. A stable and reproducible human Blood-Brain Barrier model derived from hematopoietic stem cells. *PLoS One* **2014**, *9*, No. e99733.

(29) Ravid, O.; Elhaik Goldman, S.; Macheto, D.; Bresler, Y.; De Oliveira, R. I.; Liraz-Zaltsman, S.; Gosselet, F.; Dehouck, L.; Beeri, M. S.; Cooper, I. Blood-Brain Barrier cellular responses toward organophosphates: natural compensatory processes and exogenous interventions to rescue barrier properties. *Front. Cell. Neurosci.* **2018**, *12*, 359.

(30) Aday, S.; Cecchelli, R.; Hallier-Vanuxeem, D.; Dehouck, M. P.; Ferreira, L. Stem cell-based human blood-brain barrier models for drug discovery and delivery. *Trends Biotechnol.* **2016**, *34*, 382−393.

(31) Dehouck, M.-P.; Jolliet-Riant, P.; Brée, F.; Fruchart, J.-C.; Cecchelli, R.; Tillement, J. P. Drug transfer across the blood-brain barrier: correlation between in vitro and in vivo models. *J. Neurochem.* **1992**, *58*, 1790−1797.

https://dx.doi.org/10.1021/acs.jmedchem.0c01774
J. Med. Chem. 2021, 64, 1593−1610